rAPID
WIN THE SHORT RANGE

NASA/DLR

Aeronautic Design Challenge 2018|2019

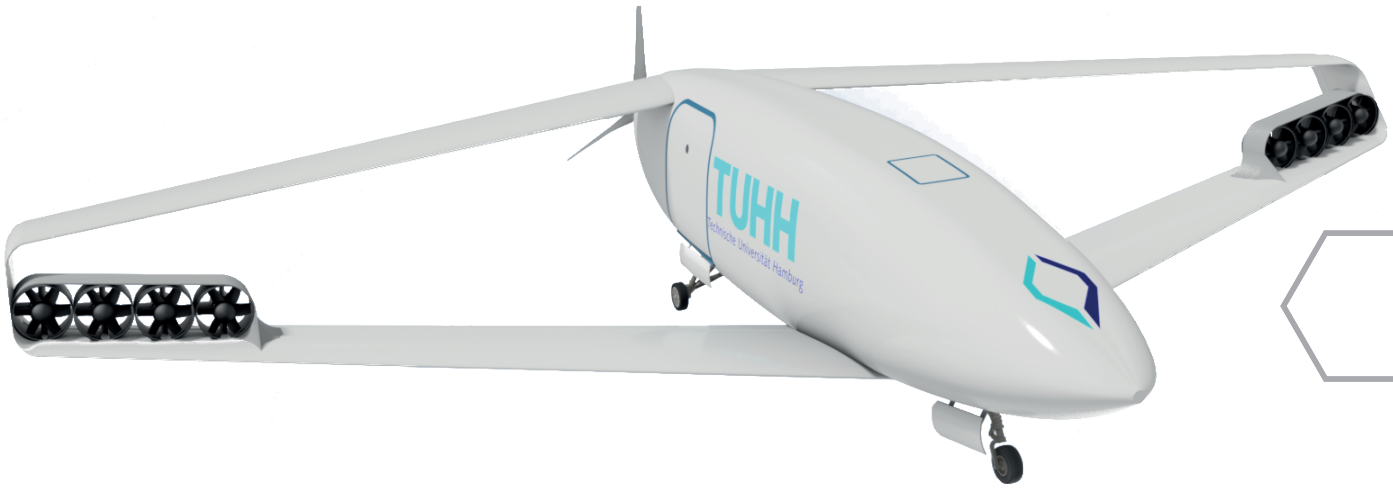

Team

Nils Külper, B. Sc. (Team Leader)
Lars-Hendrik Lemke, B. Sc.
Julian Stuwe, B. Sc.
Markus Berschik, B. Sc.
Esther Schaupeter, B. Sc.
Thomas Weber, B. Sc.

Academic Support

Prof. Dr.-Ing. Volker Gollnick

Submitted on June 30, 2019

TUHH
Technische Universität Hamburg

ILT
Technische Universität Hamburg
Institut für Lufttransportsysteme
Blohmstr. 20, 21079 Hamburg

TUHH, Institut für Lufttransportsysteme, D-21079 Hamburg

Institut für Lufttransportsysteme
Prof. Dr.-Ing. Volker Gollnick
Blohmstr.20
D-21079 Hamburg

Datum und Zeichen Ihres Schreibens	Geschäftszeichen	Hamburg,
	Prof. Dr.-Ing. Volker Gollnick	25. Juni 2019

Bescheinigung und Freigabe des Beitrags zur DLR/NASA-Design-Challenge 2019

Hiermit wird bescheinigt, daß der Beitrag der Studierenden zum Studierendenwettbewerb DLR-NASA-Design Challenge 2019 am Institut für Lufttransportsysteme geprüft und freigegeben wurde. Die Einreichung des Beitrags wird hiermit befürwortet.
Für weitere Rückfragen stehen Herr Daniel Bodmer, M.Sc. daniel.bodmer@tuhh.de oder ich gerne zur Verfügung.

Mit freundlichen Grüßen

Volker Gollnick
Institutsleiter

Postanschrift
21071 Hamburg

Besucheranschrift
Blohmstraße 20
21079 Hamburg

Telefon
+49 (0) 40 428 78-4196

Fax
+49 (0) 40 428 78-2979
www.tu-harburg.de/ilt

E-Mail
volker.gollnick@tu-harburg.de

TUHH
Technische Universität Hamburg

ILT
Institut für
Lufttransportsysteme

TUHH, Institut für Lufttransportsysteme, D-21079 Hamburg

Institut für Lufttransportsysteme
Prof. Dr.-Ing. Volker Gollnick
Blohmstr.20
D-21079 Hamburg

Datum und Zeichen Ihres Schreibens	Geschäftszeichen	Hamburg,
	Prof. Dr.-Ing. Volker Gollnick	28. Juni 2019

Bestätigung der eigenständigen Projektbearbeitung zur DLR/NASA-Design-Challenge 2019

Hiermit wird ausdrücklich bestätigt, daß

Herr Nils Külper, TUHH
Frau Esther Schaupeter, TUHH
Herr Lars-Hendrik Lemke, TUHH
Herr Thomas Weber, TUHH
Herr Markus Berschick, TUHH
Herr Julian Stuwe, TUHH

den eingereichten Projektbericht sowie alle dahinter liegenden Arbeiten vollständig eigenständig und ausschließlich unter Zuhilfenahme der angegebenen Quellen erstellt haben.
Für weitere Rückfragen stehen Herr Daniel Bodmer, M.Sc. daniel.bodmer@tuhh.de oder ich gerne zur Verfügung.

Mit freundlichen Grüßen

Volker Gollnick
Institutsleiter

Postanschrift
21071 Hamburg

Telefon
+49 (0) 40 428 78-4196

E-Mail
volker.gollnick@tu-harburg.de

Besucheranschrift
Blohmstraße 20
21079 Hamburg

Fax
+49 (0) 40 428 78-2979
www.tu-harburg.de/ilt

Abstract

The racing APID (derived from lat.: apidae = real bees) (rAPID) concept fulfills the needs for an aircraft concept for thin haul routes to rural and sub urban areas as part of the Joint NASA/DLR Aeronautic Design Challenge. This project gives an overview over the current situation in this sector including fundamental challenges and requirements like economical challenges due to many takeoffs and landings.
The rAPID is build entirely of carbon fiber reinforced plastic (CFRP) to save mass and thicknesses are validated with the finite element method (FEM). To operate on small airfields the rAPID holds a box wing for less drag and a compact design with a wingspan of not more than 15 m. The wings are optimized to ensure good and safe handling qualities. Impeller are located on its lower wings to create thrust takeoff (T/O) and ensure yaw control. A pusher propeller is located at the back for cruise flight. As a special feature for short T/O, the main landing gear is electrically driven. Energy for engines, cockpit and cabin is supplied by a turbine during cruise and a battery during on and near ground operations to ensure a quiet aircraft (A/C).
A novelty for small aircraft are the avionics and the cabin. The A/C does not hold any windows, only screens and the cabin seats are ultra lightweight and therefore, quick change devices. To reduce staff costs and to achieve autonomous flights, the avionics are of the same scope and complexity as newest commercial aircraft.
This rAPID concept is compared to the Cessna 208 Caravan (C208) in mass and performance. Therefore, T/O and landing performance and cruise speed are determined. Possible and mandatory operations, based on the rAPID concept, are presented and the costs are estimated which are lower than typical for that A/C type. This results in a better profitability for airlines.
The innovative cabin, the higher performance than competitors, lower operation cost and the ability to fly without a pilot makes rAPID the ideal concept for a new short range A/C for 2025.

The rAPID Team

Contents

List of Figures

List of Tables

Nomenclature

Formula Symbols

Latin Formula Symbols

Symbol	Unit	Meaning
A	$[m^2]$	Area
a	$[m/s]$	Sonic velocity
acc	$[m/s^2]$	Acceleration or deceleration
ae	$[s^2/m^2]$	Aerodynamic factor
b	$[m]$	Span
C	$[-]$	Coefficient
c	$[m]$	Chord length
D	$[N]$	Drag
E	$[-]$	Glide ratio
e	$[-]$	Oswald-Factor, i.e. aerodynamic efficiency
f	$[-]$	Force normalized with A/C weight
g	$[m/s^2]$	Acceleration of gravity
l	$[m]$	Length
L	$[N]$	Lift
Ma	$[-]$	Mach-number
m	$[kg]$	Mass
p	$[Pa]$	Pressure
R	$[km]$	Range
T	$[N]$	Thrust
v	$[m/s]$	Velocity
x	$[m]$	Distance

Greek Formula Symbols

Symbol	Unit	Meaning
α	$[deg]$	Angle of attack
Δ	$[-]$	Difference
γ	$[-]$	Climb gradient
η	$[-]$	Efficiency
λ	$[-]$	Aspect ratio
ρ	$[kg/m^3]$	Density

Indexes

Index		Meaning
1	=	Ground roll
5	=	Climb/approach
Avi	=	Avionics
Bat	=	Battery
BF	=	Specific fuel mass
D	=	Drag of 3D-body
d	=	Drag of 2D-airfoil
ECS	=	Enroute climb speed
EDLG	=	Electric driven landing gear
EDF	=	Electric ducted fan
ext	=	Extended
in	=	At the EDFs intake
L	=	Lift of 3D-body
l	=	Lift of 2D-airfoil
max	=	Maximum
min	=	Minimum
MU	=	Motor unit
out	=	At the EDFs outlet
PCU	=	Power control unit
r	=	At wing root
Rec	=	Rectifier
ref	=	Reference
req	=	Required
ret	=	Retracted
rot	=	Rotation
S	=	Stall
TD	=	Touchdown
TO	=	Takeoff
TR	=	Transition/flare
t	=	At wing tip
tot	=	Total
w	=	Wing
∞	=	At the far field

Abbreviations

AC	Air Conditioning
ADIRS	Air Data Inertial Reference System
ADS-B	Automatic Dependent Surveillance - Broadcast
AFDX	Avionics Full DupleX Switched Ethernet
AoA	angle of attack
AoI	angle of incidence
ARINC	Aeronautical Radio Incorporated
A/C	aircraft
CAB	central avionics bay
CFD	Computational Fluid Dynamics
CFR	Title 14 of the Code of Federal Regulations
CFRP	carbon fiber reinforced plastic
COG	center of gravity
CON/MON	Controller / Monitor
CPM	Core Processing Modul
C208	Cessna 208 Caravan
Data Comm	Data Communication System
DEP	distributed electric propulsion
DOC	direct operating cost
EAB	engine avionics bay
ECAM	Electronic Centralized Aircraft Monitoring
EDF	electric ducted fan
EFVS	Enhanced Flight Vision Systems
E2EE	end-to-end-encryption
FAA	Federal Administration Association
FEM	finite element method
FOD	foreign object damage
FPLG	free piston linear generator
Galileo	European Global Navigation Satellite System
GBAS	Ground Based Augmentation System
GNSS	Global Navigation Satellite System
GPS	Global Positioning System
GT	gas turbine
HUD	Head-up-Display
ICAO	International Civil Aviation Organization

IFE	In-flight Entertainment
ILS	Instrument Landing System
IMA	Integrated Modular Avionics
INS	Inertial Navigation System
IOC	indirect operating cost
ISA	International Standard Atmosphere
ISIS	Integrated Standby Instrument System
LCC	life cycle cost
LDG	landing gear
M	million
MAB	main avionics bay
MTOM	maximum takeoff mass
MZFM	maximum zero fuel mass
NACA	National Advisory Committee of Aeronautics
NAS	National Airspace System
NextGen	Next Generation Air Transportation System
NRC	non-recurring cost
OLED	organic light emitting diode
OME	operational mass empty
PAX	passenger
PFC	Primary Flight Computer
rAPID	racing APID (derived from lat.: apidae = real bees)
RC	recurring cost
SBAC	Society of British Aircraft Constructors
SFC	specific fuel consumption
SSB	split speed brakes
SVS	synthetic vision system
TE	trailing edge
TG	turbo generator
TLAR	Top Level Aircraft Requirements
TOC	total operating cost
T/O	takeoff
UA	Unmanned Aircraft
US	United States
USD	US-dollar
VLEO	Very Low Earth Orbit

1 Introduction

Small commuter aircraft types mainly operate on local routes with few passengers (PAXs). Therefore, only small A/C are required. Due to this type of operations, flight routes present a significant economic challenge for commercial airlines. Low PAX demand results in lower use of the aircraft which thereby increases fixed costs. Furthermore, a high frequency of T/O and landing increases operating costs. This results in higher per-seat costs and passengers might choose different means of transportation. [19][64]
It is not an option to eliminate such routes, either. Some spare communities, like several in the in Alaska in the USA, would be cutoff causing supply problems especially in emergency situations. For this purpose, the subsidy program 'Essential Air Service'was put into place in the United States (US) to ensure a minimal level of scheduled air services. [19][64][89] Goal is to gain a better alternative as the C208 which is currently the most suitable one available for this kind of operation.
Most small commuter aircraft are allowed to operate with a single pilot according to Title 14 of the Code of Federal Regulations (CFR) Part 135 which results in limitations for the A/C size. Additionally, air cargo is often operated at times with a minimum of PAX demand, e.g. at night. As such, there is an opportunity to reduce the unused time and thereby costs. [19][64]

1.1 Literature Overview

For this A/C concept many different sources were studied including books, dissertations, papers and internet documents. Every source used and quoted is listed at the end but the most important ones are the two most recent books by Raymer [72] about aircraft design.

2 Requirements Discussion

Every project has requirements which define the needs for the final product to satisfy the stakeholders. Those requirements, defined by the NASA/DLR, are called business requirements and directly influence the Top Level Aircraft Requirements (TLAR). They always consist of a unique ID, a responsible person, a threshold and goal value with a unit if applicable. If a comment for a better understanding is required, it was added. An overview of the TLARs and the achieved values by the rAPID concept are shown in chapter 7. [26][35]
In this 'NASA/DLR Joint Design Challenge'the main focus is on economical and operational feasibility as well as sustainability. As mentioned before the costs shall be as low as possible to ensure a profitable business for airlines. Therefore, the maintenance costs need to be at a minimum which is challenging for an A/C with many takeoffs and landings. The other aspect is to maximize the operational use by creating a utilization of minimum 18 h a day. This requires a smart operations plan and can be accomplished with a minimum staff cost, a double usage of the A/C (as freighter and as PAX transporter) and a very quiet aircraft. Another important and challenging aspect of the A/C is the ability to operate on very short runways with a maximum of 304.8 m during takeoff and landing to support communities with small airfields as well.

3 Conceptual Design

3.1 Methodical Approach

For this challenge the guidelines of agile project management were followed, dividing the time available into three sprints: concept freeze, parameter identification and documentation [48].
Based on the requirements provided by the challenge certain functions like complete flight mission, takeoff, landing, creating thrust and more can be found. Based on these top level aircraft functions, solutions were collected and listed in a morphological box. The possible solutions listed in the box were analyzed and evaluated based on their feasibility for a small commuter aircraft. Unrealistic options got eliminated. Afterwards, each team member individually created one or two concept ideas. Finally, those concepts were evaluated and the best concept idea was selected.

3.2 Aircraft Design

In this section a brief introduction of the special design features of the aircraft design is given for a general overview. A more detailed description of those features is presented in chapter 4. The aircraft is a boxwing configuration with a hybrid driven pusher propeller and comes along with the following special features:

- low wingspan through boxwing configuration
- less drag by omitting vertical tailplane
- high efficiency through hybrid propulsion concept
- low noise emission through full electric takeoff
- short runway length through electric driven main landing gear
- quiet and safe ground movement through electric driven main landing gear
- easy handling characteristics through full fly-by-wire technology
- extraordinary safety level through ballistic emergency chute (especially for autonomous flight)
- low cabin noise
- low structural weight through windowless design
- special passenger experience through large organic light emitting diode (OLED)-screens
- simple configuration switch (passenger to cargo)

A three side view can be seen in figure 3.1 and used key technologies are shown in figure 7.1.

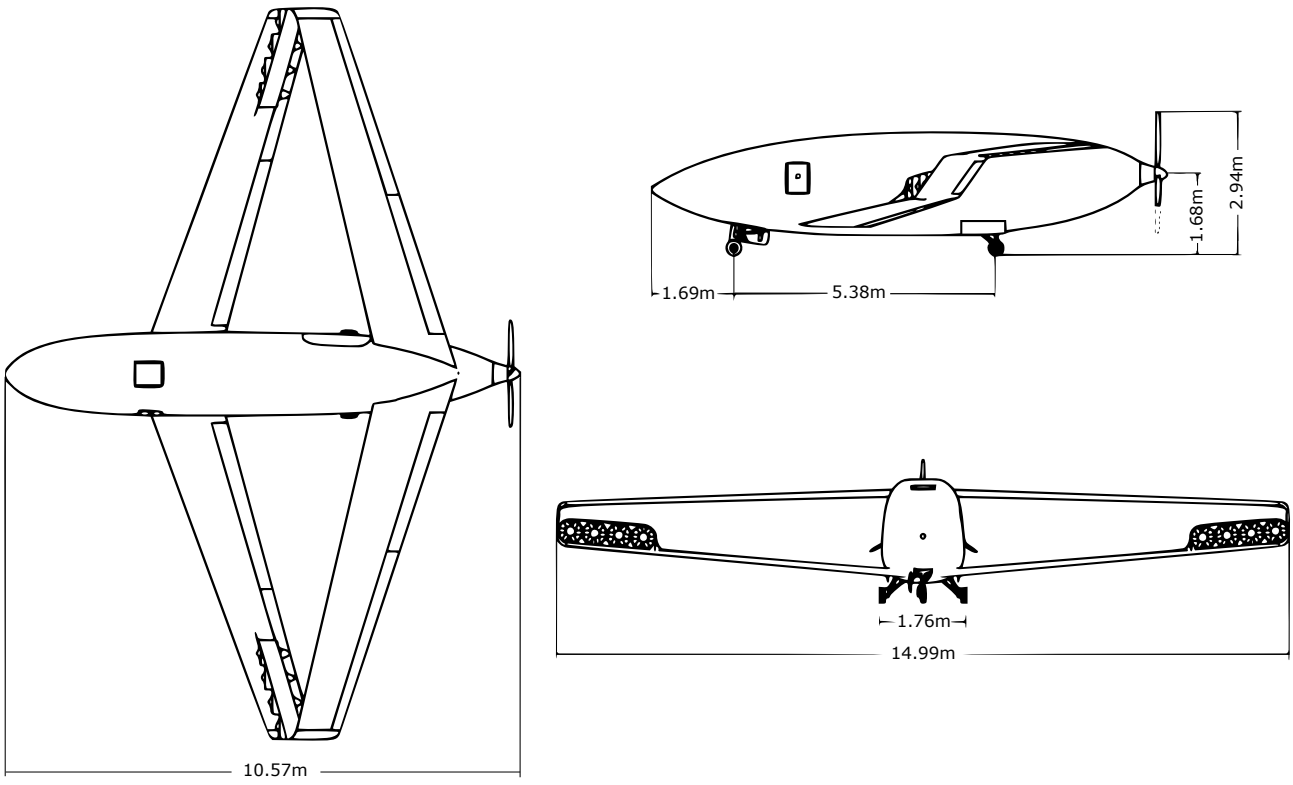

Figure 3.1: Three side view of the rAPID

4 Technical Design

In the following chapter the major technical designs of the rAPID concept are described in detail.

4.1 Aerodynamics

In this chapter the aerodynamic design for the rAPID is carried out.

4.1.1 Wing Design

The main task of the wing is to produce the necessary lift at all flight phases. The most decisive phase is the T/O. Due to the requirement for a very short runway length it is important to get airborne using a minimum speed. That results in a low stall speed requirement. On the other hand, the cruise speed is preset and efficiency at this speed plays a major role as well [19]. Therefore the wing design needs to satisfy both requirements.
The wing design procedure used in this case can be seen in figure A.2. After determining all requirements a general wing configuration and shape is chosen. In the following steps all relevant parameters of this configuration are calculated, beginning with the wingspan, due to special requirements for its maximum. Thereafter the chord lengths, sweep angle and lift ratio between both wings are assumed. For the resulting wing geometry the wing area and the required lift coefficient can be determined. In a profile comparison an airfoil suitable for the requirements is searched. If no airfoil can be found to meet the lift requirements, the chord length or the wingspan has to be adjusted until an appropriate airfoil for both, cruise and T/O, is found. Due to the high required range of lift coefficients for different flight phases, a high lift design is included into the profile comparison. After the airfoil is chosen the dihedral and the twist are estimated to provide good dynamic flight characteristics. The final design step is sizing the control surfaces in order to provide flight controls suitable for all required maneuvers. To validate the total wing design, the performance is checked against the initial requirements list.

Lift requirements and general shape. The maximum total A/C mass at T/O is estimated to be 3600 kg for aerodynamic calculations. Flight performance calculations have shown, that a stall speed of 30 m/s or less in T/O configuration is required to meet the runway length goal, see chapter 5.3. Thereby, a total lift force of $L_{tot} = MTOM \cdot g = 3600\,\text{kg} \cdot 9.81\,m/s^2 \approx 35.3\,kN$ needs to be produced. In order to minimize the stall speed the wing area needs to be large. This A/C is supposed to operate from small aerodromes, which means especially the wingspan is limited. A wing geometry that combines a small wingspan with a large wing area is the boxwing configuration. Other benefits of a boxwing are a reduced induced drag and a high efficiency compared to a standard configuration with negative lift providing horizontal stabilizers. An equal distribution over both wings, i.e. both wings produce the same amount of lift, provides the highest aerodynamic efficiency [69]. Therefore, both wings have a similar geometry. On the other hand, it is important that in case of a stall the forward wing stalls first in order to automatically reduce the angle of attack (AoA) for recovery. This can be solved by a slightly unequal wing loading of the forward and the rear wing with the COG shifted more to the front.

Wingspan. Aerodromes are categorized by the International Civil Aviation Organization (ICAO) aerodrome reference code and the Federal Administration Association (FAA) Airplane Design Group [22][40]. The wingspan together with the reference field length and the main gear wheel span determine on which category of aerodromes the A/C is permitted to land on. For code A aerodromes, which are the smallest possible, a wingspan of less than 15 m is required. The wingtip connectors require 0.2 m each, which leads to an useful wingspan of 14.6 m.

Geometric parameters for static behavior. Several iteration steps have shown that a chord length of 1.6 m at the root and 0.9 m at the tip is useful. In order to achieve pitch control and to increase the useful COG range, the wings need a separation in flight direction. Therefor, this offset is set to 5 m. This leads to high sweep angles when connecting the wingtips, such, that the forward wing has a sweep of 20 deg and the rear wing of −15 deg. The wing area is then calculated to 18.25 m^2 for each wing, using equation 4.1.

$$A_{ref} = 0{,}5 \cdot (c_r + c_t) \cdot b \tag{4.1}$$

Required lift coefficients. As mentioned above, the COG position defines the lift ratio ΔL, i.e. the amount of lift the forward wing (wing 1) produces, compared to that of the rear wing (wing 2). Using equation 4.2 and the above given stall speed requirements the required lift coefficients at the stall speed for each wing at different lift ratios can be determined. The results for sea level and ISA are shown in table 4.1. With the empty mass COG close to the aerodynamic center and the ability of arbitrarily distributing fuel over a forward and a rear wing fuel tank the COG position can be maintained in a narrow range, such, that the forward wing provides 50 % to 53 % of the total lift.

$$C_L = \frac{\Delta L * L_{tot}}{\frac{1}{2} * \rho * v^2 * A_{ref}} \tag{4.2}$$

$L_{w,1}/L_{w,2}$	$C_{L,1,req}$	$C_{L,2,req}$
0.50/0.50	1.7552	1.7552
0.51/0.49	1.7903	1.7201
0.53/0.47	1.8605	1.6499

Table 4.1: Lift coefficient requirements

Profile selection. The profile defines the shape of the wing in chordwise direction and determines the local aerodynamic quality. Besides the aerodynamic design the profile has to be designed to provide enough space for the wing structure, the flap actuation system and the fuel tanks. For this design the aerodynamic performance at low speeds is the sizing factor.
To simplify the design process only a few common airfoils were compared in detail. As this is a low to medium speed subsonic A/C design the airfoil characteristics at speeds of 30 m/s up to 100 m/s and a Reynolds number within the range of 500 000 to 11 000 000 are of interest. The National Advisory Committee of Aeronautics (NACA) provides an extensive database of tested airfoils. For this design process the four digits NACA-Series was used [2]. This system allows for a fast comparison of the impact of the most decisive parameters and thereby a fast selection of an useful airfoil. Additionally, some high-speed sailplane airfoils were compared. For the comparison the relevant operating points were calculated for each airfoil using XFoil. XFoil is a free license program for 2-D subsonic airfoil analysis and includes a four and five digits NACA-airfoil generator with the option of defining flaps [52]. Arbitrary airfoils can be loaded as well. For this analysis airfoils defined by 300 coordinate points were used. Input parameters were the airfoil geometry, flap size and location, flap deflection angle, Reynolds number, Mach number and either desired AoA or desired lift coefficient.
As mentioned in section 4.1.1 the crucial parameters of an airfoil are the maximum lift coefficient as well as the glide ratio under T/O and cruise conditions. From the required lift coefficient of the wing, requirements for the lift coefficient of the 2-D airfoil can be derived. 2-D airfoil data assumes a rectangular wing geometry with infinite span. A divergent wing geometry has an impact mainly on the lift slope $C_{L\alpha}$. This impact can be approximated using equation 4.3 [38].

$$C_{L\alpha} = \frac{C_{l\alpha}}{1 + \frac{C_{l\alpha}}{\pi \cdot \lambda}} \tag{4.3}$$

The Oswald factor e represents the aerodynamic efficiency dependent on the wing configuration. Some typical values are given by Kroo [46]. For a boxwing the factor is $e \approx 1.46$ [46]. With that adjusted lift slope the lift coefficient can be transferred with equation 4.4 [38].

$$C_l = C_L \cdot \frac{C_{l\alpha}}{C_{L\alpha}} \tag{4.4}$$

As the lift slope of the various airfoils may vary, a required 2-D lift coefficient would need to be calculated for each airfoil. To simplify this step and to keep the results more comparable the lift coefficients of the profile

analysis are directly transferred into 3-D data, using the above equations.
The airfoil NACA2409 is the thinnest one of the 4-digit NACA-Series that meets all requirements. In figure 4.1a it can be seen that the necessary flap deflections depend on the COG position and vary between 15 deg and 20 deg for the forward wing. Comparing figures 4.1a and 4.1b it becomes clear that the forward wing stalls first. When in T/O configuration the flaps of the rear wing can still manage additional deflections in both directions for flight control purposes without stalling and thus can work as an elevator.

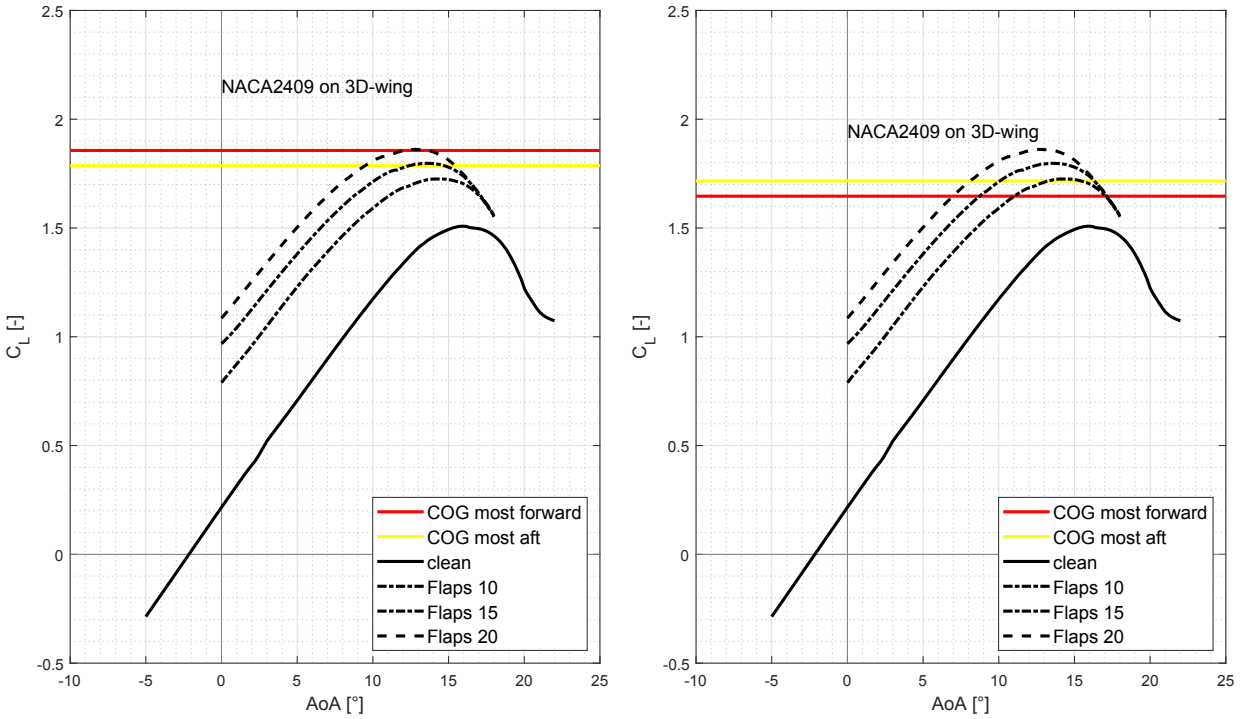

a) Forward wing

b) Rear wing

Figure 4.1: Lift coefficient of 3-D wings at 30 m/s and sea level according to ISA including required maximum for different COG positions

Geometric parameters for dynamic behavior. Some geometric parameters needed for a good behavior of the A/C are discussed on a qualitatively basis in this section. The determination of the final values for these parameters are subject of future wind tunnel and flight test, as there are many interference that may have an impact. The COG of this A/C is between both wings and maneuverability is granted by large sizes ailerons. A positive dihedral on the lower wing of 5 deg is chosen to increase roll stability. A slightly negative dihedral on the upper wing of -1.7 deg to decrease the distance between the wingtips for a more lightweight construction of the wingtip connector. [72] The angle of incidence (AoI) is set to 0 deg for the lower wing, such, that the fuselage operates at a small positive AoA in cruise to minimize down force of the fuselage. The AoI for the upper wing needs to be slightly positive to compensate the down wash effect of the forward wing. [17] This effect needs to be quantified in wind tunnel tests. A wing twist can be used to shift the region on the wing where stall occurs first. For a boxwing those regions naturally are the wingtip of the forward and the root area of the rear wing [17]. In order to maintain roll control as long as possible it is desired to shift the region of first stall of the forward wing to the root area as well. Therefore, the lower wingtip is twisted by -1 deg.

Control surfaces. Due to the fly-by-wire technology control surface deflections can be mixed for optimal handling qualities. This leads to the following assignment of control inputs to surfaces. Pitch control is provided by the trailing edge (TE)-flaps of the rear wing, roll control is provided by all TE-flaps and yaw

control is provided by differential thrust of ducted fans near the wingtip. The latter is supported by one-sided deflection of split speed brakes (SSB) in the wingtip connectors for peak performance. Flap deflections for high-lift are mixed with deflections for flight control by superposition. The lower flaps are also divided into two parts to realize slightly different deflection angle for the area effected by the yaw-fans' slipstream. A specialty of rAPID is a negative flap deflection at T/O-run to ensure high friction between the driven wheels and the runway. At rotation the flap deflection automatically changes to a positive angle. Another major feature of this A/C is the high drag configuration. Flight performance calculations have shown, that a total drag of around 4.9 kN on final approach is desired to minimize the landing distance. The A/C drag is increased to this value using the SSBs at the wingtip connectors, plus deflecting the inboard and outboard flaps of the rear wing in opposite directions and splitting the outboard flap. The additional drag coefficient ΔC_d of a SSB with 60 deg deflection each side can be estimated to 1.5 [42]. A full 60 deg deflection of the outboard flaps would produce too much drag, such that the drag can be controlled electronically for the desired value. The sizing results of the SSB in the wingtip connector can be seen in table 4.2.

lower chord length	upper chord length	height	split flap size	$C_{d,ret}$	$C_{d,ext}$
0.2 m	0.19 m	0.8 m	$0.22 \cdot c$	0.00542	1.50542

Table 4.2: Wingtip speed brake

4.1.2 Fuselage Design

The fuselage provides protected space for most systems and for the payload, i.e. passengers and cargo. The outer fuselage shape highly depends on the required dimensions and the arrangement of those systems and payloads. Therefore, the design process starts by determining those dimensions and collecting all arrangement constraints. The main systems that are to integrate are the cabin, cockpit, avionics, propulsion system, landing gear, wing-root structure and the fuselage structure itself. Decisive factors are the total system's weight resulting of wiring lengths, safety restrictions like fire containers and emergency evacuation routes and operational aspects like turnaround procedures. The goal is to keep the fuselage drag as low as possible.
In a first step a shell covering all systems with a minimal surface area is modeled.

CFD analysis. The goal of the analysis is to localize unfavorable curves and to minimize drag and aerodynamic down force of the fuselage. To minimize calculation time the fuselage was analyzed isolated, i.e. without the wings, and only one half was modeled as it is symmetric to the x-z-plane (figure 4.2). The setup of the CFD-program ANSYS Fluent was chosen in accordance to the recommendations of Armes [4] and includes a wall friction model. A detailed list of the setup parameter are shown in table 4.3. Using the results of the analysis the down force was eliminated for most common flight phases and the drag was reduced by approximately 15 % in cruise configuration by lowering the nose and slightly changing the shape of the rear cone. The new fuselage shape was then analyzed for the crucial flight phases to achieve aerodynamic information. The results for drag are written in table 4.3.

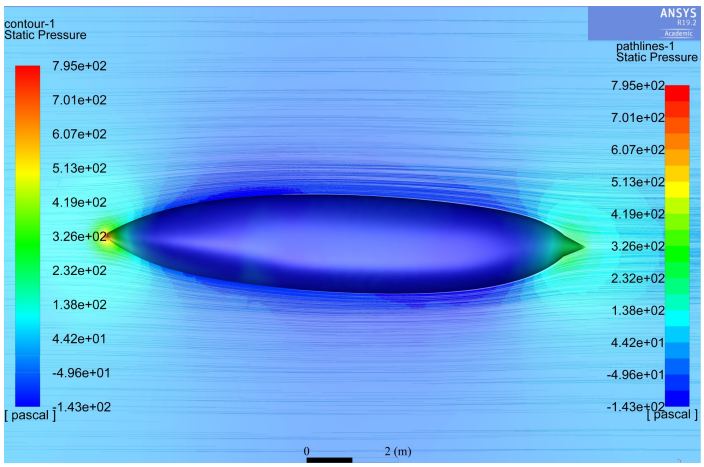

Figure 4.2: Pressure plot and pathlines on half fuselage calculated with ANSYS Fluent

T/O-run	T/O-climb	cruise	final approach
169 N	167 N	956 N	167 N

Table 4.3: Fuselage drag for different flight phases

4.1.3 Total aerodynamics

In this last step of the aerodynamic design the results of both, the wing and the fuselage design, are merged into aerodynamic parameters of the total A/C for flight performance calculations and for comparison with other A/C. These parameters are the total lift and drag coefficients and the glide ratio in different configurations. For this purpose the aerodynamic forces of all components were summed up, including an interference factor of $Q = 1.2$ for the drag [31]. The total forces are then normalized by the total wing area and the dynamic pressure to achieve the total A/C lift and drag coefficients C_L and C_D. The glide ratio is defined as $E = C_L/C_D$. The values are written in table 4.3. Additionally flaps, brakes and gear positions are given in this table for a better overview.

	Wing 1	Wing 2 Flap						
Flight phase	Flap	inboard	outboard	LDG	SSB	C_L	C_D	E
T/O-run	−10 deg	−5 deg	−5 deg	extr	retr	-0.2125	0.0221	-9.64
T/O-climb	20 deg	13.5 deg	13.5 deg	extr	retr	1.2189	0.0330	36.91
cruise	-4.9 deg	-4.9 deg	-4.9 deg	retr	retr	0.1981	0.0114	17.39
final approach	20 deg	25 deg	splitted	extr	extr	1.2189	0.16912	7.21

Figure 4.3: Aerodynamic parameters of the total aircraft (retr = retracted; extr = extracted)

4.2 Structure

The most important factors which have to be considered during the design of an aircraft structure are weight, strength and reliability. A material which meets these requirements is CFRP. Nowadays it is commonly used for the aircraft structure. Since the entry into service is planned for 2025, future materials like carbon nanotubes are not expected to be ready and affordable for mass production and the same consideration applies for bionic structures. Even though CFRPs promise a significant loss in weight, they come with the cost of loosing lightning protection. To retain this protection, it is necessary to integrate a conductive mesh like aluminum on the CFRP surface. [55]
The fuselage and wing construction is realized as a reinforced shell. The skin is reinforced by a framework of structural components, which absorb and transmit the stresses. The fuselage is made of three sections (cockpit section, middle piece and aft section). Each consist of two elements. This construction allows simple production, maintenance and repair. The aircraft is subject to fives types of stress: tension, compression, shear, bending and torsion or a combination of these. To get an optimal design of the structural components, it is beneficial to vary the number of layers and fiber orientation, regarding their applied stresses. [71] An overview about the main stresses for the structure components with the corresponding advantageous fiber orientation is given in table 4.4.

Stress	Fuselage	Wing	Opt. fiber orientation
bending	skins & stringers	skins & stringers	0° [63]
shear	skins	spar webs	± 45° [71]
torsion	skins	skins & spar webs	± 45° [5]
concentrated load introduction	bulkheads	ribs	0°
hold contour	frames	ribs	0°/±45°/90 °

Table 4.4: internal loads

4.2.1 Fuselage

The main task of the fuselage is the accommodation of the payload. The fuselage forms the main body of an aircraft to which wings, engines and gears are attached. Since the aircraft is not pressurized, the fuselage shape differs from commonly used cylindrical shape.

The more rectangular cross section provides more space for the passengers [78]. Cut-outs like windows, doors or the landing gear bay heavily disturb the flow of forces and weaken the structure. Thus, heavy reinforcements are needed to support the surrounding structure. To eliminate some reinforcements OLED screens are used instead of windows. This results in a weight-saving of about 30 % (see figure 4.4) [6].

4.2.2 Wing

The characteristic of a boxwing is the connection of two vertical separated classic wings into one. This connection is realized with a lightweight rigid joint, which does not enhance aero elastic problems because it transmits all stresses [23]. The boxwing is built with ribs and two spars at 25% and 70% chord length. The distance between the ribs is relatively high due to the strong wing shell. In order to realize a small profile thickness, the resistance to bending is increased by increasing the wall thickness of the wing box [16].

4.2.3 Landing Gear

The landing gear is designed as a common tricycle gear with two main wheels and one nose wheel. For more efficiency in cruise the landing gear is fully retractable. As the COG of the aircraft will be in between of the two wings, the main landing gear can not be integrated in a wing and needs to be fully integrated into the fuselage. Due to the electric driven main landing gear it is necessary to have reinforced landing gear rods in flight direction. Side stays ensure that the main landing gear stays in position when extended. Since the rAPID uses a pusher propeller, the landing gear needs to provide enough ground clearance to the propeller during T/O.

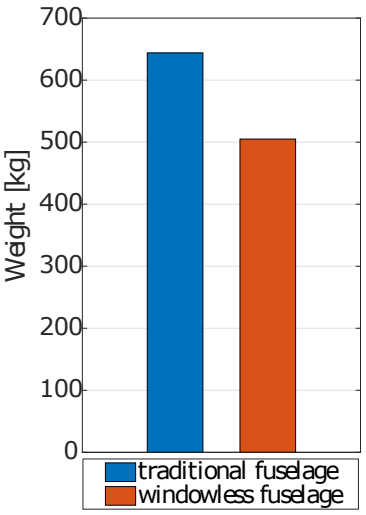

Figure 4.4: Comparison between a traditional and windowless fuselage

4.3 Propulsion And Energy

To gain system efficiency the rAPID uses the concept of a serial hybrid power train. The general idea is to size the gas turbine to an optimum and buffer spikes in power consumption with batteries, while mechanically decoupling the engine from the propulsion system. As said in chapter 3.2 the T/O is fully electric which defines the system architecture to a serial approach instead of a parallel one [51].
Thrust is generated by three subsystems. During cruise flight a propeller, located at the rear of the aircraft, acts as an efficient and reliable way to generate thrust [72]. To address the problem of over sizing the propeller to meet thrust requirements, during takeoff and climb, a set of electric ducted fans electric ducted fans (EDFs) generates additional thrust. This configuration also allows a differential thrust yaw control. To further shorten the runway length, integrated wheel motors are used in the landing gear (LDG).

4.3.1 Propulsion System

Pusher propeller. By placing the main propeller at the rear end of the fuselage propeller efficiency is decreased through the disturbed airflow in which the propeller operates but aerodynamic efficiency will be gained through the slower airflow over wings and fuselage as well as the abundance of prop wash effects [72]. The propulsive efficiency $\eta_{Prop,P}$ of a propeller in a pusher configuration suffers a loss of about $2\,\% - 5\%$ [72], while the efficiency loss due to prop wash effects of the C208, calculated with the Society of British Aircraft Constructors (SBAC)-Method is about $3\,\%$. Both aircraft therefore will operate at similar propulsive efficiency during cruise flight.

EDF. One decisive factor for placing and sizing the EDFs is the required yaw moment generated trough differential thrust. The sizing is based on a failure of two EDFs on one side of the wing while in the climb segment. Another factor is the required thrust output during takeoff and climb which should be at least $T_{EDF} = 5\,\text{kN}$ based on the calculation in Chapter 5.3. By using data of the AIRBUS E-Fan (Table 4.5) a configuration of four fans on each wing is chosen.

Fan	Diameter	Thrust	Input Power	Weight
Airbus E-Fan	520 mm	750 N	30 kW	30 kg

Table 4.5: Data of the AIRBUS E-Fan [68]

By looking at the definition of the ideal propulsive efficiency

$$\eta_{Prop} = \frac{V_\infty}{V_{in} + \frac{V_{out} - V_{in}}{2}} \tag{4.5}$$

as well as an estimated ratio of $V_{in}/V_\infty = 1.2$ on top of the wing, it appears that the EDFs are poorly placed in terms of optimizing their propulsive efficiency $\eta_{Prop,EDF}$. A more suiteable place would be right under the wing where $V_{in}/V_\infty = 0.7$ [32]. However, regarding the short duration of the takeoff and climb segment and the EDFs main purpose to generate thrust during this segment, a placement where the EDFs are protected from foreign object damages (FODs) and noise is shielded by the wings is more important.

Electric driven LDG. The electric driven LDG as the third propulsive system further decreases the runway length by accelerating the aircraft during the takeoff roll. While running on wet concrete the system is designed to generate a thrust of $T_{ELDG} = 10\,\text{kN}$. With little friction effects nearly all of the provided shaft power will be transferred into thrust. The propulsive efficiency is almost 100 %.
It must be taken into consideration that using a driven LDG on contaminated or non asphalted runways, slipping effects can cause serious FODs at the propeller or even fuselage [68]. To counteract this problem mudguards are used. Additional use of the system can be made during taxi to reduce battery drain and noise emissions [83]. Furthermore, by providing differential torque an active nose gear steering is not necessary.
Thrust-to-weight ratios T/W for relevant flight segments of all three systems combined are presented in table 4.6.

	Take off roll	initial climb	final climb	cruise
T/W	0.49	0.21	0.21	0.11

Table 4.6: Thrust to weight ratios

4.3.2 Efficient Power Generation

To find the most suitable engine or system to generate energy several concepts are compared. A conventional [10] and a recuperated [85] turbo shaft engine, called turbo generator (TG) are compared to a turbo diesel engine [20] as well as a free piston linear generator (FPLG) [33][75] in terms of fuel efficiency, system weight and the corresponding runway lengths. Fuel cell systems have been proven to be too heavy for its usage in short duration flights [44].
Rubber engine sizing is used in some extend to scale the engines up to the required power output of about 400 kW during cruise (see chapter 4.3.3). In comparison to a conventional turbo generators, a recuperated TG is 20 kg heavier due to the heat exchanger. The specific fuel consumption (SFC) is reduced by 15 %. [85] The Textron Lycoming LTS 101-650B1 serves as a reference gas turbine (GT). Due to technical progress, improvements of 13 % can be assumed [85].
Table 4.7 presents engine data as well as corresponding values for fuel consumption of a 99 min flight mission with the aircraft masses given in 5.2.

	Turbo generator	Turbo generator (recup.)	Turbo diesel	FPLG
SFC [kg/kWh]	0.289	0.257	0.2	0.195
Weight [kg]	100	120	408	450
Specific power [kW/kg]	4.14	3.45	1.04	0.92
Fuel consumption [kg]	319.2	305.7	301.6	303.2

Table 4.7: Engine data comparison

Based on the challenging T/O requirements a high specific power is required. In table 4.7 it can be seen that only a turbo generator can fulfill the TLAR. A recuperated TG is selected due to the lower noise emission and higher efficiency. This engine, compared to the C208's turboprop engine, is estimated to be about 20 % more fuel efficient.
Starting the TG requires 56 Nm [36]. The synchronous electric generator on the turbine shaft is also used as the turbine starter by using a bidirectional inverter.

4.3.3 Energy Storage And Distribution

The key factor for designing an efficient electrical architecture (figure 4.5) is using components that operate with little power losses. With promising developments of inverters based on siliconcarbide a high efficiency and small system weight is realized [74]. The same applies to motor efficiency, which by now is reaching up to 95 % [79]. Depending on the short time frame until 2025 the predictions of upcoming technologies strongly vary. Therefore only established concepts are chosen and an increase of 5 % power/energy density as well as an increase of 1 % efficiency are added to the values given in table 4.8.
While operational voltages often are limited to 540 V due to partial discharge effects, improvements in insulation technologies as well as the low flight altitude allow higher voltage limits resulting in less cable weights and higher component power densities [45].
The battery has to be sized such that at all operation conditions including error cases enough power is available to ensure a safe condition of the aircraft. The power flow from the battery to the aircraft during TG-off mode is described in equation 4.6.

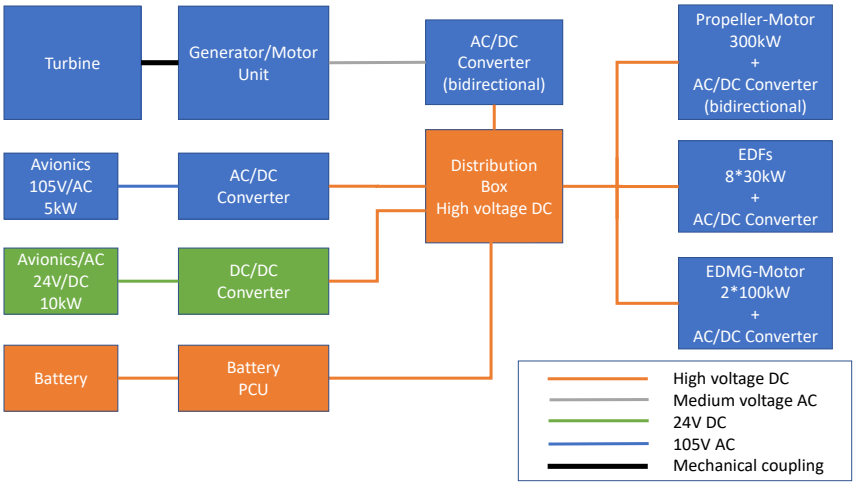

Figure 4.5: System architecture

Component	Efficiency by 2025	Power density by 2025 [kW/kg]	Ref.
SiC-inverter	0.98	30	[74]
Rectifier	0.99	30	[49]
Motor units	0.96	7	[79]
Generator	0.96	7	[67]
Battery+PCU	0.96	5.25	[34][73]

Table 4.8: Properties of electric components

$$P_{Bat} = \frac{1}{\eta_{PCU}} \cdot \left(\frac{1}{\eta_{MU}} \cdot (P_P + P_{ELDG} + P_{EDF}) + \frac{1}{\eta_{Rec}} \cdot P_{Avi,105VAC} + \frac{1}{\eta_{DCLink}} \cdot P_{Avi,24VAC} \right) \tag{4.6}$$

The resulting power output reaches a maximum of about 655 kW during takeoff run. Batteries of current automotive applications are focusing on high energy densities while operating with power densities at 300 W/kg.

This would result in an unacceptable battery mass of about 2200 kg for the rAPID. Instead, a trade-off between a lower energy density and a much higher power density is taken. In 2015 Hitachi introduced a battery with a power density of 5 kW/kg and an energy density of 80 Wh/kg [34]. Considering possible values of 5.25 kW/kg in 2025 the battery weighs 82 kg. To ensure safety, a battery weight of 100 kg is chosen. The energy capacity therefore is $E_{Bat} = 8.4$kWh while a start requires $E_{Bat} = 4.3$kWh.

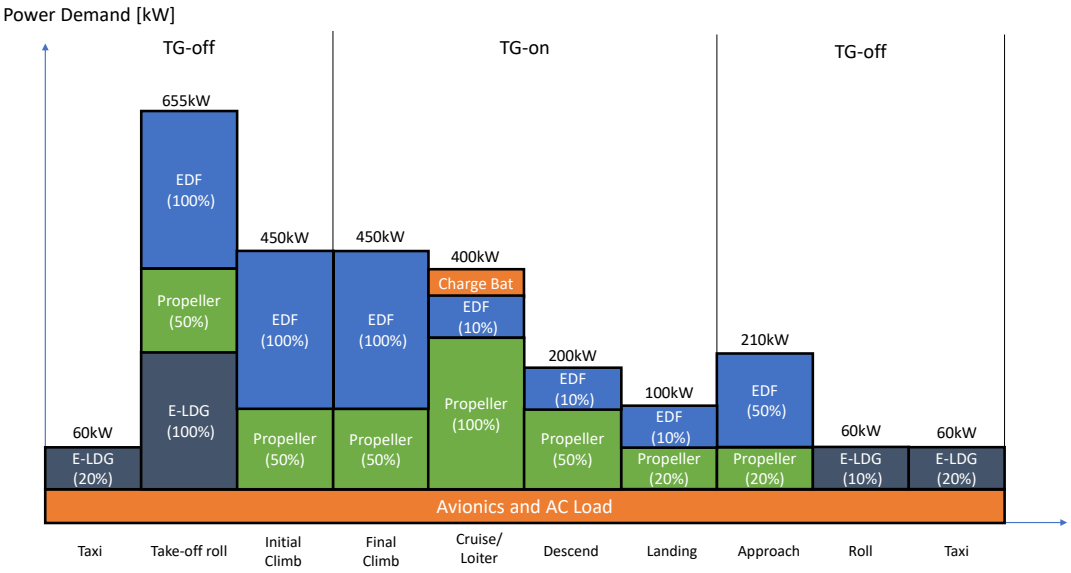

Figure 4.6: Energy demand during flight cycle

The estimated values in figure 4.6 show the power level for each system during the flight cycle. The required power output as seen in the systems architecture (figure 4.5) multiplied with the corresponding duration and load factors as described in figure 4.6 of the engine-off flight segments leads to a minimal energy capacity of $E_{Bat} = 200$ kWh. the battery is fairly overdimensioned regarding its capacity thus enabling a safety margin.

4.3.4 Acoustics

For the reduction of noise emissions a distributed electric propulsion (DEP) concept as well as a full electric T/O are utilized, eliminating the engine noise until a flight level of 400 ft is reached. By then the TG's noise is less compared to a turbo prop engine because it is more shielded. It is stated that using a recuperated GT further decreases the TG's noise through damping effects [57].
A pusher configuration usually generates more external and less internal noise emissions because the propeller rotates in a disturbed airflow behind the aircraft [66]. However, it is stated that this mostly happens due to exhaust gas flows in turbo prop A/C like the Piaggio P.180 Avanti [66]. By placing the EDFs at the outer part of the wing these disturbance effects are further minimized.
During takeoff roll and initial climb the propeller operates at a lower power setting and can be operated in a low-noise mode with a decrease in noise of about 12 dB(A) [7].
In comparison to the C208, generating 73 dB(A) during overflight [21], the rAPID is estimated to emit less noise, using the presented noise reduction strategies.

4.4 Avionics

As the commercial use of small aircraft is really costly, pilot costs should be as low as possible. This can be achieved by easy and intuitive A/C controlling or even unmanned flights. To ensure a safe flight of the aircraft, strong safety margins in form of the probability of failure safety requirements per flight hour need to be met

[62]. Systems like the control of ailerons and elevators or the autopilot, which lead in case of a failure to a catastrophic outcome, need to have a probability of failure of $< 1 \cdot 10^{-9}$. It is therefore necessary to have multiple redundant fault tolerant systems, not only regarding hardware but also software. [62][81]
The software is therefor designed to receive DO-178B Level A approval published by RTCA [3].
An abstract of the used avionic components with its wiring is shown in figure 4.7. The whole overview is shown in figure A.3.

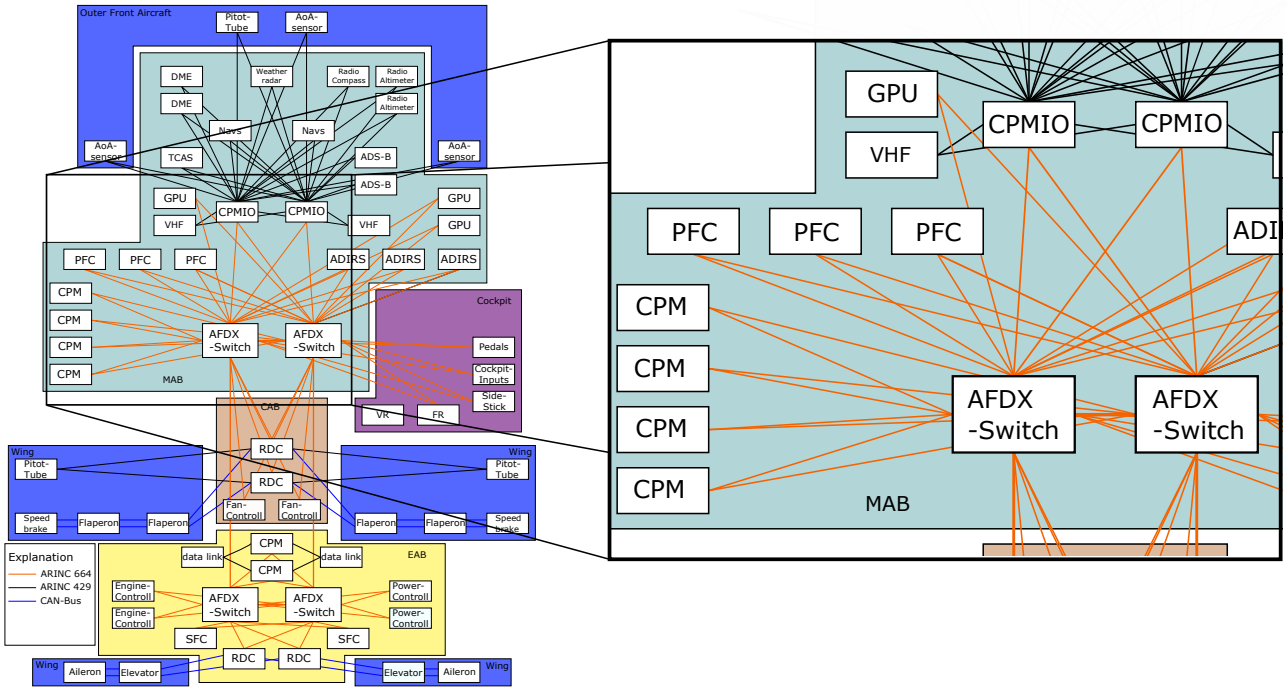

Figure 4.7: Part of the overview of avionics configuration, showing the connection of main communication backbone and PFC / CPM

All avionic components are located in three different protected areas. The main avionics bay (MAB) in front of the cockpit, the central avionics bay (CAB) and the engine avionics bay (EAB) in the back of the A/C.
The concept uses a triplex CON/MON voter architecture for the primary flight computer with two redundant secondary flight computer in the EAB [62]. Both flight computers are developed directly for this A/C to cope with the unusual boxwing configuration and reduce mass of the components. Even if one flight computer has a failure, the system is still operational. In the unlikely event that all three primary flight computers fail, the secondary flight computers take over with reduced functionality and simpler control laws, to still land the A/C safely.
To reduce development and certification costs the avionics design uses already existing and commonly used components. For communication an Aeronautical Radio Incorporated (ARINC) 664 Standard Avionics Full DupleX Switched Ethernet (AFDX) network is used, which provides the main communication link from the front to the back of the aircraft [61].
To reduce costs, Integrated Modular Avionics (IMA) based processing modules are used for other important task in the A/C, e.g. fuel control, door lock or climate control. The big advantage of IMA processing modules is that it can be used as a general-purpose computing resource, which is cheaper than hardware specialized systems for every single task and can handle robustly partitioned application software. [62]
Three redundant Air Data Inertial Reference System (ADIRS) combine the measured data of the external AoA sensors, pitot-static-tubes and inertial navigation systems Inertial Navigation System (INS) with Global Navigation Satellite System (GNSS) signals [37][62]. AoA sensors and pitot-static-tubes are used to measure side slip and AoA. Both sensors are actively heated to avoid icing. The overall location of the sensors are shown in figure 4.8.
Further systems are shown in A.3. Additional equipment is used to receive data via a satellite data link, described in chapter 4.7. For every control surface two redundant linear electric motors are used. Additionally,

to the main AFDX network, every actuator has an independent digital data line to each flight computer, which ensures control even if the AFDX network is compromised.

4.5 Cockpit Design

The cockpit of the rAPID is a uniquely designed concept, which provides an easy way to control the A/C by a single pilot. It is designed to reduce the workload for the pilot as much as possible without losing the situational awareness.

4.5.1 Configuration

The pilot sits in the left seat and has all important peripherals in his range. The rAPID's uniquely designed cockpit is windowless. And the pilot is therefore surrounded by a 180 deg OLED display, which shows the outside view. The image data is produced by multiple cameras and combined in three redundant operating graphical processing units. On top of the outside view, additional information will be augmented into the display. To cope for display loses, the OLED display is split into four smaller displays. As input peripherals, the pilot controls the aircraft with a side stick, pedals and thrust levers. Additionally, the pilot has a 3-D mouse to select options on the display and a keyboard for other inputs. An overview of the cockpit is shown in figure A.4.

4.5.2 Windowless Design

At the first glance a windowless cockpit looks counterintuitive to safety and comfort for the pilot. With no direct visual information, the pilot is completely reliant on his board computers and can not see what happens outside the aircraft. Introducing different cameras, which are already in use, e.g. in the A380, a strong and robust avionics system and fusing all information together, gives this visual information back to the pilot. [62][81]

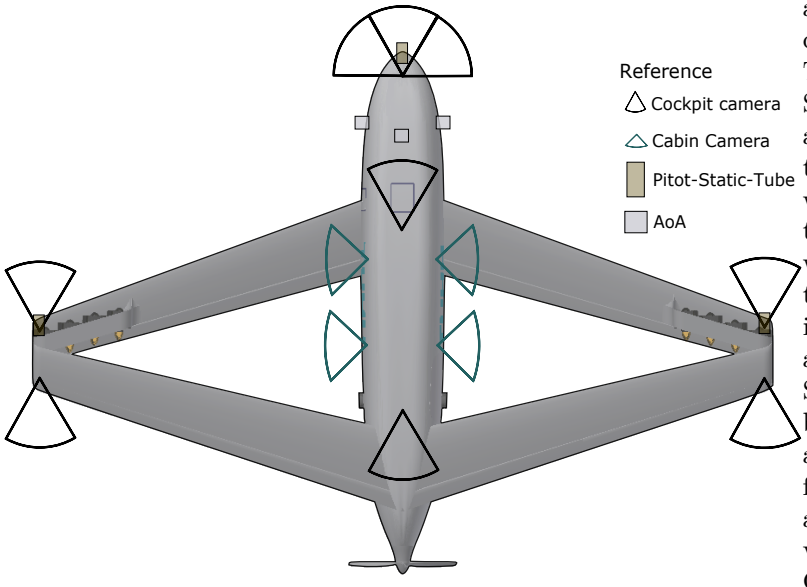

Figure 4.8: Top view of the aircraft with cameras and sensor location

Benefits occur through an overall weight reduction, reduction in SFC up to 2% and additional airport capacity in bad weather conditions [24].
Through the Enhanced Flight Vision Systems (EFVS) the pilot gets additional augmented information, which enhances the visibility at nighttime or at bad weather conditions [62]. Combined with the use of a synthetic vision system (SVS) with an augmented 3D-terrain view, the vision of the pilot will be further improved. Companies like FalconEye are trying to certify a Combined Vision System approved for CATIII conditions by the end of 2020 [56]. As an overlay a Head-up-Display (HUD), with primary flight, navigation and weather data is augmented into the displayed outside view, see figure A.5 and A.4.
Compared to the use of virtual reality glasses, all these augmentations can be easily included into the visual information from outside the aircraft, because of the existing fix points in the viewing area.

The display can be configured by the pilot, so that the comfort of using this advanced system can be maximized.

In case of an emergency, information of the occurred fault will be shown on the display in addition to the resulting checklist for fixing this problem. Thereby the workload in extreme situations can be reduced. [24]
In addition to the information on the display, redundant systems like an Integrated Standby Instrument System (ISIS), a navigation display and Electronic Centralized Aircraft Monitoring (ECAM) system is provided, in case the main display fails, see figure A.5.

4.6 Cabin Design

For the examined A/C the cabin is of particular importance as it is supposed to be a quick change A/C, i.e. the passenger version is converted into a cargo version within 60 minutes and vice versa. Hence, it is important to consider the need for an easy and quick (dis)assembly and therefore a lightweight and simple interior which also contributes to low acquisition and fuel costs.
Apart from its practical characteristics the appearance and comfort of the cabin should be taken into account since the cabin itself can be a decisive factor for passengers and airlines. A detailed view into the cabin is shown in figures A.6, A.7 and A.8 in the appendix.

4.6.1 Layout

The cabin layout is designed in a 2-abreast seating arrangement with economy seats and consists of four rows. The seat for the ninth passenger is the so-called jump seat. It is placed next to the pilot seat and can be used for either one passenger or for a teaching pilot.
One emergency exit on each side is necessary to operate it in agreement with the rules of the FAA [90]. Nevertheless, the designed A/C has a total of three emergency exits which results from the cargo version. Due to the decreasing height of the cabin from rear to front, a big entrance at the rear of the cabin with a small window is essential to enable the loading of spacious cargo from the back. That door is also used for (de)boarding. Another small exit door with a small window is on the opposite side of the cabin, behind the pilot's seat. This door is essential for the pilot to enter when flying cargo, since the cabin aisle will be full of cargo. Since the Pilot will not be able to reach the back door in an emergency, a second exit within the range of the pilot is needed to fulfill the requirements of the CFR 23 [90]. Therefor, an emergency hatch near the cockpit in front of the cargo load is installed.

Dimensions

The cabin needs to provide space for seating as well as load devices and cargo nets to transport freight. A cargo net is also used for securing the passengers' luggage since it ensures an adjustable safe and low weight placing. Assuming that the devices carrying freight can be adjusted to the A/C, formulae for economic and minimum dimensions of a PAX cabin are used to define the dimensions of the cabin and the seats [29][90]. The cabin is not pressurized. Therefor, the cabin does not need to have a circular cross section and the actual final width and height were influenced by the aerodynamics. The rAPID's cabin dimensions in millimeter are shown in figure 4.9. The cabin length is based on seat pitch, bulk cargo area and exits [65].

4.6.2 Seats

A key technology of the rAPID is represented by the 'lightest and most durable aircraft seat ever', a concept from the aircraft seating manufacturer Mirus [60].
This 3.8 kg seat is made from carbon fibers (see appendix A.9). Though the seat is still only a concept, it is already 16G proven. For a final certification there still remain fire and toxicity tests to be carried out which is likely feasible until 2025.
It is a very convenient seat, especially regarding the daily (dis)assembly of the cabin. For changing the PAX cabin into a cargo version, these seats become a key factor for an economical and quick change. Due to the low

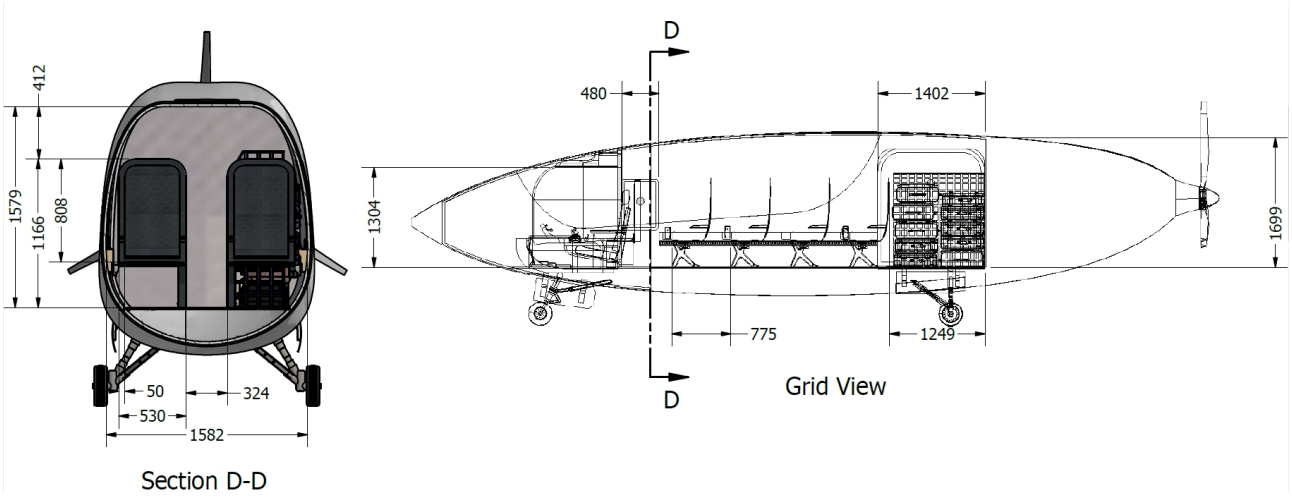

Figure 4.9: Cabin dimensions in millimeter

weight this can be done in only a few minutes by a single person. The seat may not be the most comfortable aircraft seat but in general, passengers will not be seated for much longer than 99 minutes.

4.6.3 OLED Windows

Another key technology of the rAPID are the OLED screens which are used instead of windows. They show the exterior view through cameras at the exterior fuselage (see. figure 4.8). They can also be used as an In-flight Entertainment (IFE) system.
In the first design approach a canopy window over the whole cabin was contemplated. But OLED windows are a convincing key factor for the aircraft, especially due to the weight savings and the solar protection. Table A.2 in the appendix displays the pros and cons of OLED windows and a canopy. In case of emergencies the OLED screens are supplied by the battery. Alternatively, fluorescent stripes on the floor guide the PAX to the exits.

Passenger Acceptance

A cabin without windows is a big change for passengers. One may assume that they will not buy tickets for such an aircraft because they might feel claustrophobic.
According to a survey, every third PAX fears of flying. But only 4,5 % of all respondents state that they actually suffer from claustrophobia during flying. In the same paper, in which the acceptance of a blended wing body cabin was reviewed, the participants were asked if they could accept a video system which substitutes real windows. Especially with additional functions like 'various, select-able perspectives as well as a digital zoom, navigational information and video-on-demand', the participants tend to accept the replacement.[91] Since this survey was executed in 2004 it can be assumed that results are even more promising in 2025, with a rising enthusiasm in technology.
Since 2018, the first virtual windows are already in the air. The first class cabin of Emirates'newest Boeing 777-300ER aircraft offers a realistic outside view for passengers sitting in the middle having no actual window. As first reviews state it is a remarkable and exciting passenger experience which provides 'incredibly clear'views [25][76].
Apart from that, many new A/C concepts include the idea of a windowless cabin. On top of that the 'Crystal Cabin Award 2018'went to Airbus's windowless cabin [15].
All things considered, especially taking into account the promising studies, it can be assumed that the passengers will quickly accept and even enjoy the new windowless passenger cabin.

4.6.4 Equipment & Air Condition

According to FAA regulations a flight attendant is essential from 19 PAX seats or more [90]. Thus, the rAPID is operated without a cabin crew.
As the A/C is designed to fly only short ranges within a maximum time of 99 minutes and to fly very economical, galley and lavatory are not installed. Consequently, the change can be carried out quick and by only one person. A widely used alternative in general aviation, a portable urinal/funnel, could be offered by the operating airline. It can also be used for motion sickness [82].
The Air Conditioning (AC) is an evaporative cooler which is commonly used in such non-pressurized small aircraft [88]. It is designed in such a way that it can provide individually warmer or cooler air than the room temperature, adjustable by every PAX.

4.7 Unmanned Aircraft

In order to achieve the high economic goals of the concept, in a first step unmanned cargo flights will be considered for nighttime. In the future remotely controlled passenger missions are considered.
Unmanned aircraft (UA) will have to share the controlled and uncontrolled airspace with conventional manned aircraft. Therefore, Unmanned Aircraft (UA) need to be integrated into the same airspace.
The FAA is pushing its National Airspace System (NAS) the Next Generation Air Transportation System (NextGen) to full realization until 2025. Part of the strategy is the digital transponder system Automatic Dependent Surveillance - Broadcast (ADS-B). The system has benefits over older transponder systems, due to its higher availability and coverage. [87]
Furthermore, NextGen enhances air to ground and ground to ground communication with its Data Communication System (Data Comm). This overall benefits the flight planning and improves navigation, accuracy, communication and surveillance. A new 4-D flight pass is resulting from the improvements in strategic planning, which reduces flight duration and waiting times due to other traffic or weather. [87]
Another key point for UA is the use of stable data links to communicate and control the aircraft. To control an aircraft directly via this data link the most relevant requirements are low latency (round trip of 2 s for 95% of messages), high continuity (delivery probability of 99.999%) and high availability. [70] Currently no commercial satellite communication system meets these requirements, with a small and compact low weight solution. [14][53][59]
The most promising satellite communication approach of different companies is the satellite constellation of SpaceX, called Starlink [41]. It consists of 11927 satellites in Very Low Earth Orbit (VLEO). The satellite connection will have a latency of just $50 - 70$ ms with a bandwidth per user of around 1 GB/s. [30][43][54] Half of the constellation will be in orbit in March 2024 and therefore fully functional in 2025. The first internet connection should be established in the end of 2019 [80]. Through the great amount and the very low orbit of the satellites in the constellation, these antennas will be reasonable small, comparable to the antenna build by cobham with a mass of roughly 5 kg [14].
A typical unmanned cargo mission will start with the connection of an external pilot onto the A/C. The pilot will check all systems and programs the route into the flight computer of the A/C. The overall mission will be split into three parts, takeoff, flight and landing. In all phases a direct data link is established using the Starlink network. In the takeoff phase the controller has direct access onto the visual information from all cameras, additional to all system information. After the A/C is airborne, it enters the flight phase in which the autopilot is used to fly certain predefined way points. The pilot is permanently in contact with a controller and receives all status information of the A/C. The flight information will be transmitted on the one hand side, by the Starlink data link and additionally through the redundant ADS-B System. If necessary, the pilot has direct access onto the visual information of the cameras.
In the landing phase the A/C uses its internal navigation systems to fly near the airport. For bigger airports with certified CATIII Instrument Landing System (ILS) the A/C is using this information to land. For smaller airfields an external GBAS is needed to land the UA. The general purpose of the system is to reduce the error of the GNSS data through atmospheric disturbance and the actual location of the A/C. The ground system sends the calculated error from the exact position to the A/C, which then can calculate its actual position without the disturbance. [9] A general overview over the GBAS is given in figure 4.10.

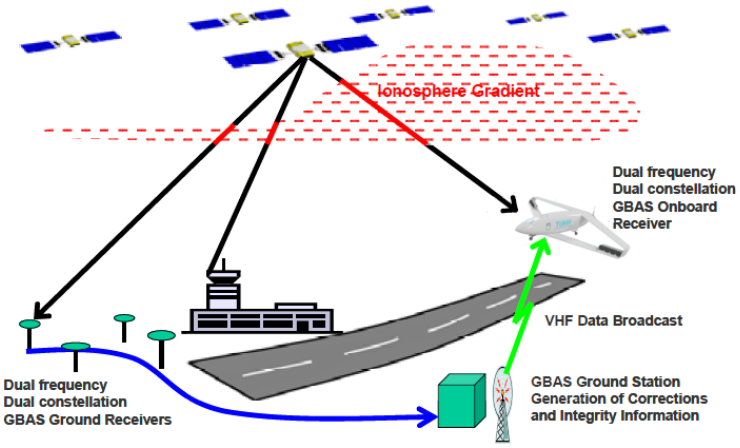

Figure 4.10: GBAS Architecture, based on [8]

Studies show that with data fusion of different GNSS, e.g. Global Positioning System (GPS) and Galileo will provide enough information to land in CATIII conditions [8]. In the near future this system will be ready and certified for the use in CATIII conditions and therefore for autonomous landings. With the certification of this system, other airfields with a working ILS will soon install a GBAS due to its lower operation and maintenance costs. [9]
The external pilot will need to sit in an office with protected a data link to the A/C. To cope with occurring errors during flight, the autopilot is designed as a fail operational system, refer 4.4. Even if the connection of the pilot is interrupted, the A/C can takeoff, fly and land autonomously. The pilot is therefore only for surveillance purposes connected with the aircraft, but can always interrupt the system.

Because the whole communication and control of the aircraft is realized by a wireless connection, the probability of signal jamming or spoofing needs to be considered. While in normal flight signal jamming is rather unlikely due to the height of the aircraft, whereas jamming at takeoff or landing is more likely. In the takeoff phase the autopilot can takeoff without constraints, whereas the landing phase is more problematic. If all signals are jammed, the aircraft returns to a defined holding position. The rAPID ensures that if there is no way the pilot can reconnect to the A/C after a certain time, the parachute abort system is activated and the aircraft lands safely in the defined holding zone.
The communication via internet needs to be encrypted carefully. Therefore, a common end-to-end-encryption (E2EE) needs to be used. To achieve a secure system the secret key for the encryption needs to be securely changed after every flight. Additionally, incoming data packages from the data link are processed through a protection gateway, which decouples the outer world from the A/C [11]. With this encryption signal spoofing is practical not possible, because no viable information package with the used encryption can be inserted into the communication.
It will still be a challenge to protect the aircraft data link from all possible threads and therefore more research in this area is needed.

5 Flight Performance

5.1 Design Range

For both PAX and freight configuration a minimum range of 370.40 km (200 nm) is required but a higher range would be appreciated. An airline which operates in this sector is 'Cape Air' which operates in the US. 67 % of the airlines missions in the USA are shorter than 100 nm which is equivalent to 185.2 km. Furthermore, all of their missions are not more than 416.7 km (225 nm) in length. As a result, a cruise range R_{plan} of 550 km is selected to reach even further locations. [12][84]

5.2 Aircraft Mass

System	Mass	Unit
avionics & cockpit	290	kg
structure & LDG & wheel eng.	1100	kg
cabin & AC	170	kg
power generation	170	kg
battery	100	kg
power electronics & fuel sys.	65	kg
actuator	140	kg
propulsion	220	kg
parachute	20	kg
OME	2255	kg

Table 5.1: Final masses of the sub systems

The A/C mass contains of an operational mass empty (OME) which is driven by the A/C components and systems, the fuel mass m_{fuel} and the payload m_{pay}. This results in the maximum takeoff mass (MTOM). The weight assumed for the components and the resulting OME are listed in table 5.1 and detailed mass identifications are listed in B.1.
A typical operation is defined by the fuel needed for the mission like climb or cruise and the reserve like cruise to alternate. With an OME of 2255 kg the specific fuel mass can be determined for each segment based on the Breguet range equation which is rewritten in formula 5.1 to determine the mass.

$$\frac{m_i}{m_{i-1}} = e^{\left(\frac{-R \cdot SFC \cdot g}{v \cdot (L/D)}\right)} \tag{5.1}$$

The specific fuel mass m_{BF}/MTOM is the product of each segment times a factor of 3 % for unusable fuel mass. The payload is 997.9 kg according to the TLAR including one pilot. This results in the maximum zero fuel mass (MZFM) which is the sum of OME and payload. [28]

With these values the MTOM is determined iterative, being the sum of the payload, fuel mass and the OME. The resulting values are listed in table 5.2. These are shown in figure 5.1 compared with the C208. It can be seen that the rAPID is slightly lighter due to new technologies even tough it contains of a hybrid system and a boxwing. [28][71]

Variable	Value	Unit
$m_{payload}$	997.9	kg
MZFM	3252.9	kg
m_{fuel}	285.4	kg
MTOM	3538.3	kg

Table 5.2: Mass share

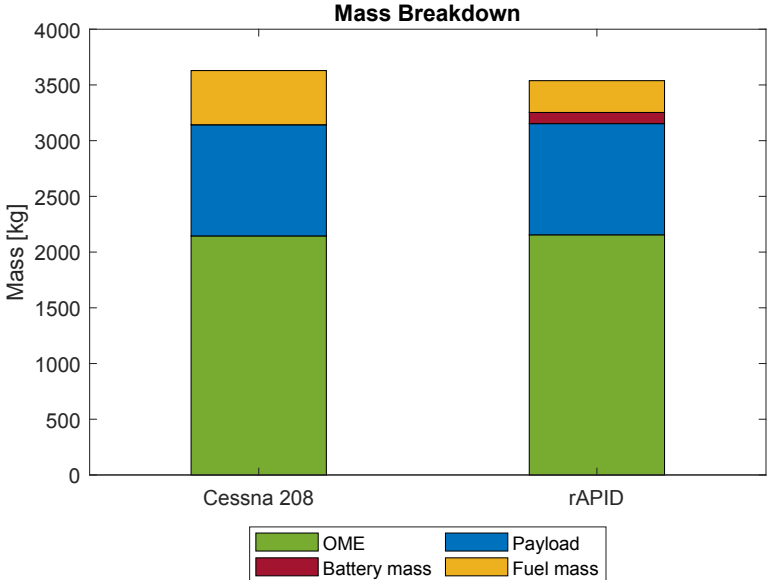

Figure 5.1: Mass Breakdown (based on [86])

An A/C never just operates at its design range but in fact, the ranges and masses on board may vary. It is assumed that the max. payload is 1100 kg due the small cabin volume. A Mass-Range-Diagram is determined by calculating, first, a payload-range-diagram and then adding the MTOM values. Therefore, the range is determined for points: P1 (max. payload), for P2 (max. fuel mass) and P3 (zero payload). Those three points are calculated by using the Breguet range equations for each state. The results are shown in figure 5.2. The bold black line represents the never exceed weight which is the MTOM. [28]

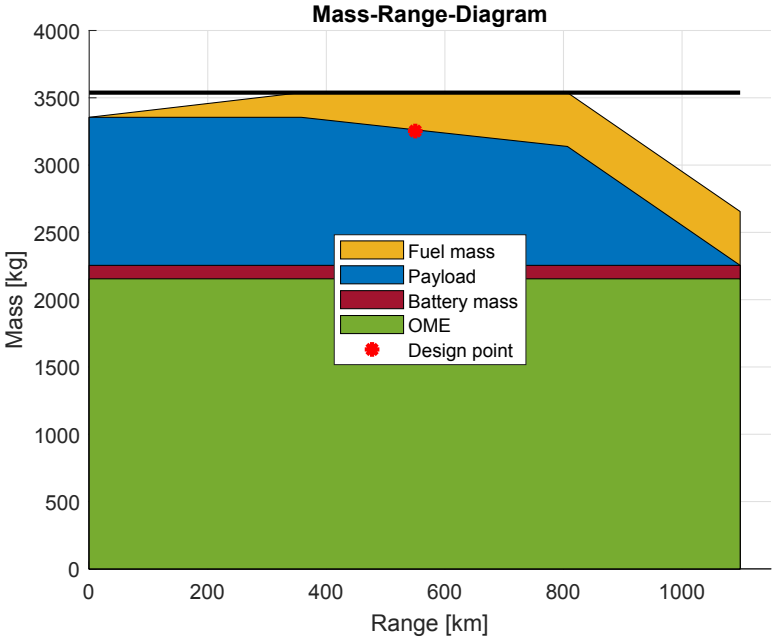

Figure 5.2: Mass-Range-Diagram of rAPID

5.3 Takeoff And Landing

Distances needed for T/O and landing are calculated the same way because 'landing is like takeoff only backward[s]' [71]. The process, of one of these two, can be divided into four segments until an obstacle height of 10.67 m is cleared: roll on ground, A/C rotation, transition/flare and initial climb/final approach [72]. The ground roll is determined using the medium acceleration or deceleration between halt and lift off speed $v_{TO} = 1.1 \cdot v_S$ for T/O or touchdown speed $v_{TD} = 1.15 \cdot v_S$ for landing. Because the wheels are electrically driven and down force is applied, the main thrust on ground is created by the wheels. The down force ensures that contact with ground is maintained even on uneven runways. An aerodynamic factor ae contains the drag influence dependent on the square of the velocity. The acceleration or deceleration

$$ac_{i,ji} = g \cdot (f_{ji,propeller} + f_{ji,wheels} + ae \cdot v_i^2) \tag{5.2}$$

is determined for zero velocity and lift off or touch down speed with the forces created by the propeller, EDFs and the wheels normalized with the weight. The ground roll distance can be found:

$$x_1 = \frac{1}{2 \cdot g \cdot ae} \cdot \ln\left(\frac{b_{2,02}}{b_{0,02}}\right) \tag{5.3}$$

The aircraft rotation is assumed to take 1 s and the distance therefore is x_{rot} [72]. The next phase is the transition in which the A/C accelerates to 1.2 times stall speed which is also the climb speed v_2. During landing the aircraft decelerates from approach speed $v_a = 1.3 \cdot v_S$ to touch down velocity. The climb rate is needed for both the transition and climb.

$$\gamma_{climb} = \sin^{-1}\left(\frac{T_{climb} - D}{MTOM \cdot g}\right) \tag{5.4}$$

The transition distance x_{TR} is determined by multiplying the radius with the sinus of the climb rate. If the obstacle height of 35 ft is cleared during transition, the distance traveled during climb x_5 is zero and only the transition distance is determined. If not, the distance traveled during climb $x_5 \neq 0$ and both distances must be determined. This applies equally to landing.
All relevant distances for T/O and landing, including the total distance needed x_{tot}, are listed in table 5.3. It demonstrates that rAPID stays within the limits given by the requirements.

Parameter	Takeoff	Landing
γ_{climb}	14.3 %	-14.1 %
x_1	127.1 m	87.4 m
x_{rot}	33 m	34.5 m
x_{TR}	86.3 m	98 m
x_5	31.3 m	26 m
x_{tot}	277.7 m	246 m

Table 5.3: T/O and landing distances

Therefore, the rAPID concept has a shorter required runway then a C208 [86] and due to the redundant propulsion system, a loss of e.g. one EDF is not critical. The altitude of an airport has a mayor effect on the takeoff and landing distance. Therefore, it is required in the 14 CFR Part 23 to show these performance data for an airport altitude from sea level up to 10 000 ft. The A/C concept is not allowed to fly over 8000 ft since no pressurized cabin is used and the cabin altitude should not exceed this height.

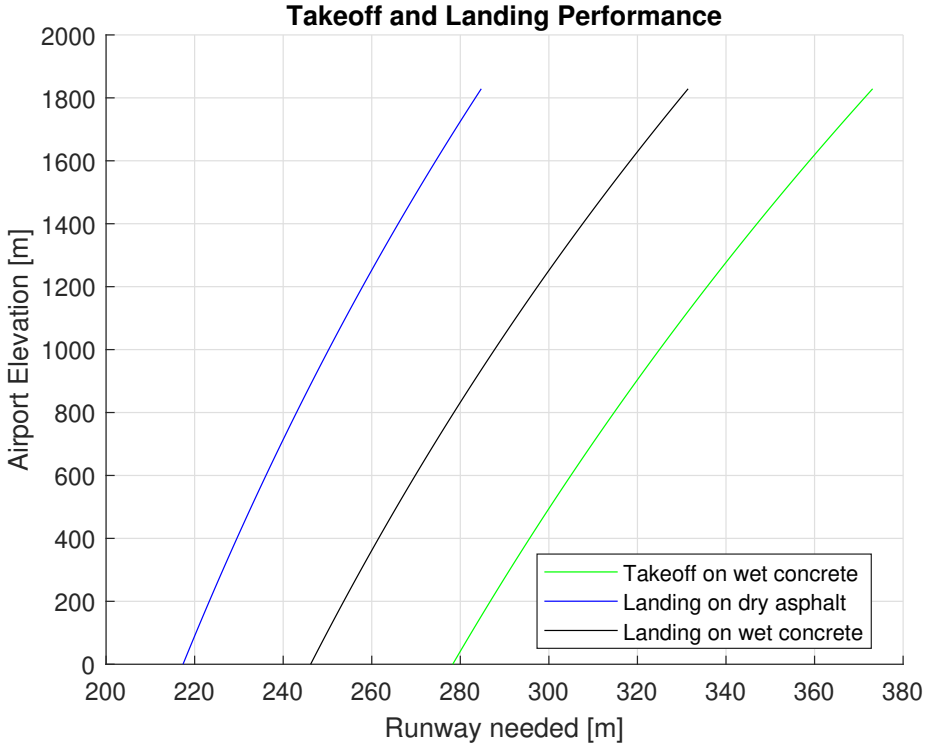

Figure 5.3: Takeoff and landing distance on different surfaces with an increasing airport elevation

After takeoff the steady climb starts at 400 ft and to ensure a good safety margin the aircraft is not allowed to perform a normal T/O or landing above 6000 ft. The increase of those distances are shown in figure 5.3. The highest airport elevation possible within the limits, given by the TLAR, is around 800 m for landing and around 500 m for takeoff. 94 % of all airports worldwide, with concrete or asphalt runways over 100 ft, have a length of more than 380 m [58]. Therefore, the A/C is able to operate on the majority of airfields, even if those are located at an elevation up to 6000 ft above sea level.

5.4 Cruise Speed

The aircraft cruise speed is important because it has an influence on e.g. the aerodynamics and therefore, the time needed for each mission segment must be determined. Those segments are:

- takeoff including initial climb until the obstacle height is cleared
- climb to cruise altitude:
  - ▷ second climb segment with v_2, LDG down and T/O thrust until 400 ft
  - ▷ acceleration at 400 ft from v_2 to $v_{ECS} = 2 \cdot v_2$ while the gas turbine is started and from there on, it is used as the energy source
  - ▷ final climb segment with v_{ECS} until the cruise altitude of 8000 ft is reached
- cruise
- descent with a selected angle of $\gamma = -4°$ until an altitude of 1500 ft is reached
- approach from 1500 ft to obstacle height with an approach gradient of $\gamma = -14.1\,\%$ based on equation 5.4
- final approach from obstacle height and landing until halt

The time, that the A/C is allowed to fly from point A to point B, is limited to 99 min. Therefore, the time needed for each segment and the range covered, are determined using basic physics. This results in a remaining time and range, as part of the planed range, for the cruise flight and therefore, a speed needed to comply with this: the cruise velocity, which in this case is ≈ 99.6 m/s. [72]

6 Operations And Cost

6.1 Operations

The rAPID is an aircraft which can be operated independent of a network structure like hub-spoke or spoke-spoke. It only needs a base with a well-equipped infrastructure which is needed for cabin change and maintenance.

6.1.1 Ground Operations

To accomplish a mission, different operations need to be done while the aircraft is on the ground. These are listed and explained further in the following.

Battery and fuel. An access to unleaded JET A-1 is necessary. The fuel pipe does not need to be a high pressure line, since the aircraft is fueled from the topside of the lower wing. An electrical energy supply either by ground power vehicles or via cables providing 230 VAC is convenient but not essential, since in general the battery is charged enough during the flight for running the air condition on ground and for the next takeoff. For safety reasons the battery is charged via the right wing and the aircraft is fueled via the left wing, i.e. there is a great distance and a simultaneous energy supply can take place.

Passenger and baggage handling. Cleaning staff and Catering is not necessary for the A/C. The baggage is stacked and unloaded by the passengers themselves with the guidance of the pilot in the therefor intended space opposite the entry door. The pilot will secure the baggage with a cargo net after boarding. Since the door functions as a ramp, there are no stairs needed. The (de)boarding times are each estimated with two minutes, since there is only a maximum of nine passengers (de)boarding the aircraft. Before takeoff, a two minute safety instructions video needs to be displayed on the OLED screens.

PAX/Cargo change. It is intended that the cabin is converted every day from a PAX cabin to a cargo cabin within 60 minutes and vice versa at the airline's base [19]. The rAPID is designed conveniently for this purpose by the use of ultra-light passenger seats. This is the main interior which needs to be (dis)assembled. The seats are secured via two latches, one connected with the seat track on the floor and one with the seat track on the side which is connected with the cabin wall. Due to the lightweight of the seats and the fast and easy (un)locking, the eight seats are (dis)assembled within approximately eight minutes. The jump seat is heavier and is not supposed to be removed regularly. Nevertheless, if there is an overload, the jump seat is still quick and easy to (dis)assemble within approximately three minutes.

Cargo handling. The freight mission is mainly supposed to be unmanned. Therefore, at least one worker is needed at the airports to (un)load the A/C. In case of a pilot personally flying the aircraft he/she could be responsible for the cargo (un)loading. The cargo load devices, designed to fit perfectly into the A/C, have small rolls underneath to ease the transport on the ground. In the aircraft they are latched on the seat tracks. For bulk cargo, nets are available to latch almost anywhere in the cabin. The cargo handling time is variable and mainly depends on the amount of bulk cargo. The turn around time for the cargo mission is preset with 30 minutes [19]. Hence, a cargo handling time of 15 to 20 minutes seems to be realistic.

Flight preparations. The pilot needs to do pre-flight checks before every flight which include the outside check and ensuring the proper function of the systems. It will not be necessary to execute route and navigation planning as in common aircraft since NextGen with Data Comm (see chapter 4.7) takes up that job [87]. The entire flight preparations are estimated with six minutes.

Maintenance. In general, maintenance work is performed at the base, where a full maintenance service is ensured. With a preset utilization of 300 flights per year and up to eight hours of ground time at the base (see chapter 6.1.2), there will be plenty of time for maintenance. Though the A/C will likely need more maintenance as regular aircraft, since it is flying only short ranges, which results in more takeoffs and landings.

Unmanned flights. For unmanned flights the same ground operations take place as for flights with a present pilot. Due to the missing pilot someone else is essential to do the work the pilot would have done according to the flight preparation listed above. For future autonomous flights with passengers one would need to handle the passenger and baggage supervision.

6.1.2 24 Hours Mission

The A/C is characterized by the double mission ability. Setting up an exemplary 24 hours utilization schedule, as shown in figure 6.1, it appears that the aircraft can operate with eight legs (light blue) carrying passengers and four legs transporting cargo (pink). These numbers arise from the preset factors from the DLR [19] as turnaround times (45 minutes PAX mission (green), 30 minutes cargo mission (dark blue)) and ground times (due to maintenance, cleaning and curfews (orange) or cabin change (yellow)). The amount of legs per mission and day need to be even-numbered so that the cabin can be changed at the base. The airborne time was calculated with the average speed from chapter 5.4 and a range of 120 nm which results in 37.02 minutes. This number is rounded to 40 minutes as a buffer. With such a 24 hours mission 2400 block hours are flown yearly.

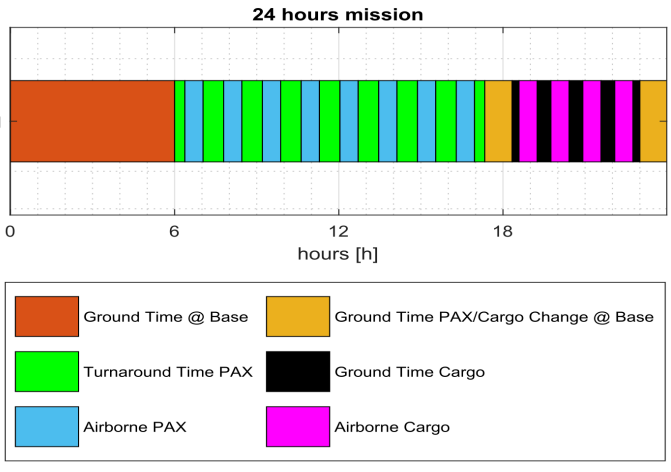

Figure 6.1: 24 hours mission

6.2 Costs

The rAPID is designed to improve the profitability of small A/C flying short ranges. An estimation of the life cycle cost (LCC) of one aircraft is presented in 2018 US-dollar (USD). Building on that, the change in costs for totally autonomous operations are specified.

6.2.1 Life Cycle Costs

Due to the very little published data (confirmed by Langhans [50]) of LCC (factors) of A/C programs the costs will be determined empirically, some analytically and some have to be best-guessed.
Manufacturer costs can be expressed as non-recurring cost (NRC) and recurring cost (RC). OME, engine thrust, max. available speed, aircraft type (business, commercial), number of engines, and technology factors influence the NRC [50]. The rAPID's development cost (NRC) are estimated with 190 M USD with the data from [50] and a regression line (see figure 6.2). The NRC of the Lilium program is estimated with 150 M USD by taking [18]. The NRC of the C208 is guessed based on the low innovation factor on a linear line with the ERJ 135 and the A319.

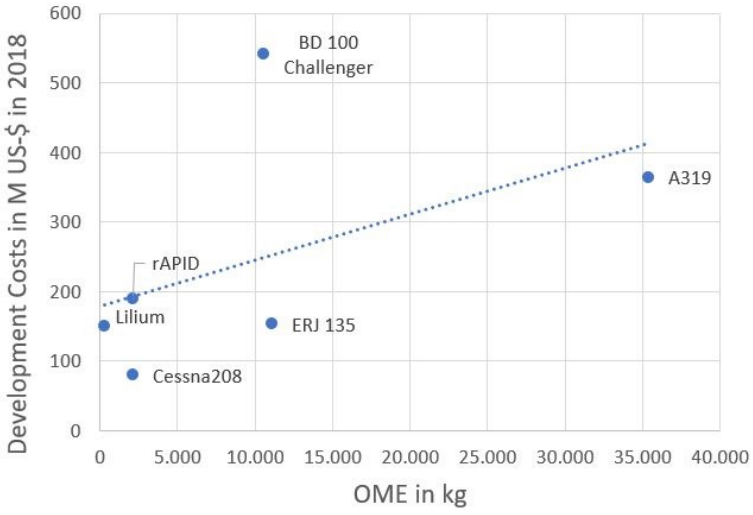

Figure 6.2: NRC in million USD in 2018 over OME in kg

The RC is approximated with the correlation of NRC, RC and the aircraft's price. Latter can be approximated with the approach of Raymer [72] which determinates the price by the OME. Accordingly, general aviation aircraft cost about 200 USD and business about 800 USD per pound. Since the rAPID is far more complex than a general aviation A/C (due to the avionics) but does not fly at high speeds and is unpressurized unlike business jets, the cost is set to 700 USD per pound. This results in a unit price of 3.15 M USD. Substituting the NRC over 800 units [19] from the aircraft price, the RC come to about 2.91 M USD. A key factor for the airline's revenue is the direct operating cost (DOC) [47]. To achieve profit, the airline needs to keep it as low as possible.

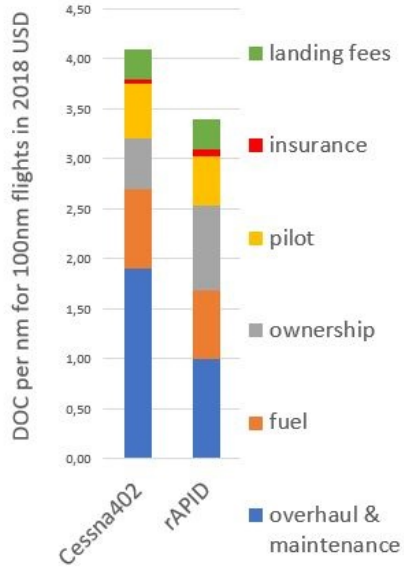

Figure 6.3: DOC

Latter is taken as a reference aircraft since it is commonly used for such missions the rAPID is designed for and data is avaiable from Stoll [84].
In figure 6.3 the difference in DOC per 1 nm for a 100 nm flight of the rAPID and the Cessna208 is presented. Fuel (0.68 USD for the 100 nm mission [39]) and maintenance cost which contribute the most to the DOC, apart from ownership [50] as well as crew costs are relatively low. Insurance costs per year is generally 1% of the aircraft's price [50]. Breaking that down by 2400 h per year, with 120 nm per mission, the insurance costs come to about 0.075 USD per nautical mile for a 100 nm flight. Landing fees are assumed with 0.30 USD per nautical mile.
To calculate the price/km/seat the indirect operating cost (IOC) need to be taken into account. According to Gollnick [27], the IOC are roughly 40% of the total operating cost (TOC). The factors are commonly distributed in the IOC as shown in figure C.1 in the appendix [77]. Since the rAPID offers almost no passenger service the IOC is lower than usual and consequently it is set to 35% of the TOC. Therefore, the price/nm/seat comes to 0.58 USD/nm/seat (0.31 USD/km/seat) which is almost 20 % cheaper than the C208.

6.2.2 Cost Estimation For Totally Autonomous Operations

In case of future totally autonomous flights, i.e. not only transporting cargo but also passengers without a present pilot, the entire cockpit will be removed. The avionics remains in the aircraft, including the flight- and voice recorder as well as the radio communication system and the parachute.
Unmanned flights will lead to a significant cost reduction, mainly since the OME is reduced by 80 kg and the salary for the pilot who will fly the aircraft from the ground can be reduced by approximately 20%. Further, the revenue is increased because of the new available space for one more passenger seat and approximately 15% more cargo. This results in an estimated profit increase of 13%.
Nevertheless, autonomous flights with passengers also imply disadvantages, e.g. the passengers are on their own and need to have access to the parachute tripping device which can be encroached. Also, the passenger acceptance is questionable since a wireless connection may always be hackable. Further, this technique is problematic in terms of ethic aspects, since a person flying the A/C who is not actually inside it with the passengers may not do his best work and bring the A/C with the PAX into danger. Hence, the avionics need to be designed so that it can not be encroached. On top of that, the machine should not be the last decision factor. It will be a challenge to do so.

7 Conclusion

This project was started to create a concept which is designed for short, thin-haul routes to rural and sub urban areas as part of the Joint NASA/DLR Aeronautic Design Challenge. The rAPID fulfills those needs by keeping all threshold requirements. Those are marked light green in figure 7.2. In some cases, the rAPID overachieves the threshold requirements and those are marked with a strong green in figure 7.2. The used key technologies are shown in figure 7.1.
All in all, the rAPID is optimized for short routes and is a great A/C for thin-haul, short range flights in 2025. As part of this, it is built mainly of CFRP to save weight. Furthermore, to operate on small airfields it holds a boxwing for less drag and a compact design with a wingspan of 15 m. EDFs are located on its lower wings to create thrust during T/O and ensure yaw control. A pusher propeller is located at the back for cruise flight. A specialty of the rAPID is that for short T/O and better ground handling the main landing gear is electrically driven. Energy for engines, cockpit and cabin is supplied by a turbine during cruise and a battery during on and near ground operations to ensure a quiet A/C.
Revolutionary is that the A/C does not hold any windows, only screens and the cabin seats are ultra lightweight and therefore are quick change devices. The avionics are designed to enable autonomous flights to reduce staff costs to a minimum. If compared to competitors like the C208, the rAPID has a better flight performance with significantly lower fuel consumption and can be operated more flexible. Even though, it has a high initial price, the rAPID has operations cost of around 28 ¢/km/person and is therefore competitive to other means of transportation [1].
It is recommended to do further studies in this A/C sector and to further develop rAPID in detail to improve parameters like costs and the aerodynamics.

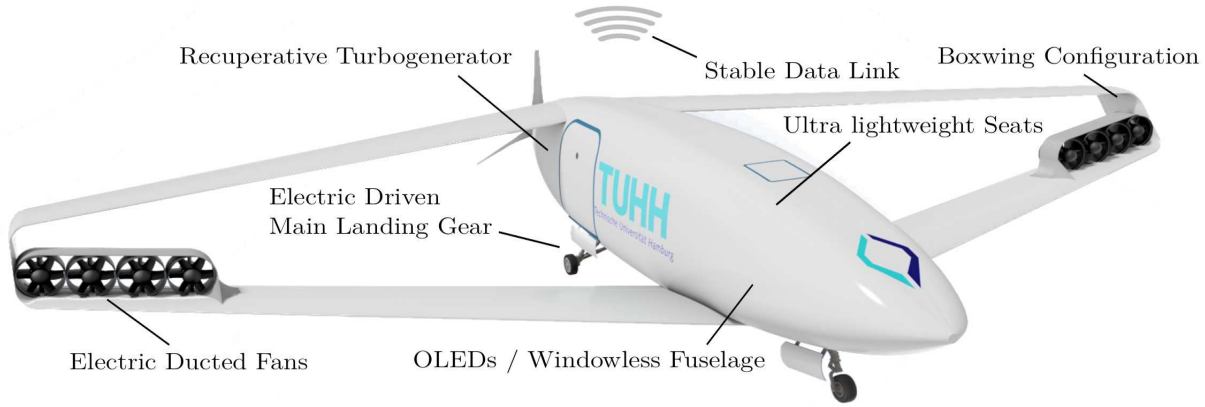

Figure 7.1: Key Technologies

Top Level Aircraft Requirements							
ID	Description/Name of requirement	value				unit (phys.)	comment
		Threshold	Goal	rAPID	C208		
R1	**Mass**						
R1.1	number of PAX	9	∞	9	9	-	
R1.2	mass (PAX + luggage)	898.11	∞	898.11	898.11	kg	
R1.3	mass of payload (freight)	907.18	∞	907.18	-	kg	
R2	**Change PAX to freight config. and backwards**						
R2.1	duration	60.00	0	60	-	min	
R3	**Number of pilots**						
R3.1	during training	2	-	2	2	-	
R3.2	flight with PAX (close future (5-10 years))	1	-	1	1	-	
R3.3	flight with freight	1	0	1	1	-	Goal = selfpiloted flight or only ground control (like UAV)
R3.4	flight with PAX (farer future (~25 years))	0	-	0	1	-	
R4	**Range**						
R4.1	aircraft in PAX configuration (9 PAX)	370.4	926	550	N/A	km	
R4.2	aircraft in freight configuration	370.4	926	550	-	km	
R5	**Flight duration and speed**						
R5.1	max. time to reach destination	99	0	99	99	min	
R5.2	speed limit below 10.000ft MSL	250	0	194.6	185.7	KIAS	
R6	**Fuel and energy reserves**						
R6.1	distance to alternate after balked landing/rejected landing	92.6	185.2	92.6	N/A	km	
R6.2	loiter time at alternate	45	∞	45	45	min	with cruise flight performance
R7	**Takeoff and Landing**						
R7.1	Takeoff length	304.8	76.2	277.7	626	m	
R7.2	Landing distance	304.8	76.2	246	495	m	
R8	**Engine**						
R8.1	Pb free fuel	-	-	-	-	-	
R9	**Cabin**						
R9.1	cabin altitude	≤2438.4	0	2438.4	2438.4	m	
R10	**Acoustics**						
R10.1	noise level of aircraft	80	65	<73	73	dB(A)	according to 14 CFR Part 36, Appendix G
R11	**Mission**						
R11.1	occupied days per year per aircraft	300	-	300	300	d	
R11.2	PAX missions:						
	- average flight distance per day	222.24	∞	222.24	222.24	km	with 9 PAX per 12h/day with max. speed according to #6
	- Turnaround	45	0	45	45	min	per flight only one turnaround time
	- round number of flights per day			Yes	Yes		
R11.3	freight mission:						
	- average flight distance per day	222.24	∞	222.24	222.24	km	with freight per 6h/day with max. speed according to #6
	- Turnaround	30	0	30	30	min	per flight only one turnaround time
	- round number of flights per day			Yes	Yes		
R12	**Life cycle cost**						
R12.1	NRC	-	0	190	80	M US-$	according to 2018 in US-$
R12.2	DOC: US-$/km/seat	~0.5-1	0	0.31	0.38	US-$	flight with 9 PAX; according to 2018 in US-$
R12.3	Demand	800	∞	800	N/A	-	number of aircrafts to be sold
R12.4	estimation of cost DOC with autonomous flight	-	0	0.27	-	US-$	just as a bonus calculation -> just goal no threshold

Figure 7.2: Requirements list and rAPID's performance (based on [13][19][64][86])

Bibliography

[1] ADAC, ed.: *ADAC Autokosten-Rechner*. 2019. URL: https://www.adac.de/infotestrat/autodatenbank/autokosten/autokosten-rechner/default.aspx.

[2] AirfoilTools.com, ed.: *Airfoil Tools*. URL: http://airfoiltools.com/.

[3] Ákos Horváth: *Standards in Avionics System Development (Overview on DO-178B)*. URL: https://inf.mit.bme.hu/sites/default/files/materials/taxonomy/term/445/13/13_CES_DO-178B.pdf.

[4] Armes, Robert: "Aerodynamic Fuselage Design and Engine Integration for the Vampire Light Sport Aircraft". Master thesis. North Carolina: North Carolina State University, 2013.

[5] Astasari, Astasari; Sutikno, Sutikno, and Wijanarko, Wahyu: "Bending and Torsional Characteristics of Carbon Fiber and Balsa Wood Sandwich Composite". In: *IPTEK Journal of Proceedings Series* 0.2 (5.2017). DOI: 10.12962/j23546026.y2017i2.2270.

[6] Bagassi, Sara; Persiani, Franco, and Lucchi, Francesca: "Aircraft Preliminary Design: a windowless concept". In: *5th CEAS Air & Space Conference 2015*. URL: https://aerospace-europe.eu/media/books/CEAS2015_211.pdf.

[7] Berton, Jeffrey, ed.: *Low-Noise Operating Mode for Propeller-Driven Electric Airplanes*. DOI: 10.2514/6.2018-3599.

[8] Boubeker Belabbas, Patrick Remi, Michael Meurer: "Galileo Performance Assessment for CAT III GBAS". In: *ENC GNSS 2008*. URL: https://www.researchgate.net/publication/224998970_Galileo_Performance_Assessment_for_CAT_III_GBAS?enrichId=rgreq-55f1ed2c786e3f68ca9e008b1c426b92-XXX&enrichSource=Y292ZXJQYWdlOzIyNDk5ODk3MDtBUzoxMDQ3OTkxODU5MzIyOTNAMTQwMTk5NzQ4MTM3Mw%3D%3D&el=1_x_2&_esc=publicationCoverPdf.

[9] Boubeker Belabbas: *Ground Based Augmentation System (GBAS)*. URL: https://www.dlr.de/kn/desktopdefault.aspx/tabid-7567/12810_read-32118.

[10] Bräunling, Willy J.G.: *Flugzeugtriebwerke: Grundlagen, Aero-Thermodynamik, ideale und reale Kreisprozesse, Thermische Turbomaschinen, Komponenten, Emissionen und Systeme*. 3., vollst. überarb. u. erw. Aufl. VDI-Buch. Berlin, Heidelberg: Springer-Verlag Berlin Heidelberg, 2009. ISBN: 978-3-540-76368-0. DOI: 10.1007/978-3-540-76370-3.

[11] BSI: *M 4.101 Sicherheitsgateways und Verschlüsselung*. 2013. URL: https://www.bsi.bund.de/DE/Themen/ITGrundschutz/ITGrundschutzKataloge/Inhalt/_content/m/m04/m04101.html.

[12] Cape Air: *Commuter Airline Perspective: On-Demand Mobility and Follow Up Workshop*. URL: http://www.nianet.org/ODM/ODMTuesdaypresentationsFinal/13WolfFINALCapeAirNASAODMConferencedeckv7MAR16.pdf.

[13] Cenek, Peter; Jamieson, Neil, and McLarin, Maurice: *Frictional Characteristics of Roadside Grass Types*. Neuseeland. URL: https://www.academia.edu/27081538/Frictional_Characteristics_of_Roadside_Grass_Types.

[14] cobham: *Cobham Announces Successful AVIATOR UAV 500 Proof of Concept*. 2019. URL: https://www.cobham.com/communications-and-connectivity/aerospace-communications/cockpit-and-cabin-connectivity/news/cobham-announces-successful-aviator-uav-500-proof-of-concept/.

[15] Crystal Cabin Award Association, ed.: *The Crystal Cabin Award: International award for excellence in aircraft interior innovation*. 2019. URL: http://www.crystal-cabin-award.com/finalists-winners/overview.html.

[16] D. Schiktanz, D. Scholz: "Box Wing Fundamentals - an Aircraft Design Perspective". In: *Deutscher Luft- und Raumfahrtkongress 2011*. URL: https://www.fzt.haw-hamburg.de/pers/Scholz/Airport2030/Airport2030_PUB_DLRK_11-09-27.pdf.

[17] Daniel Schiktanz: "Conceptual Design of a Medium Range Box Wing Aircraft". Master thesis. Hamburg, Deutschland: Hochschule für Angewandte Wissenschaft, 2011.

[18] *Deutscher Luft- und Raumfahrtkongress 2011*. URL: http://www.dlrk2011.dglr.de/.

[19] DLR: *Joint NASA / DLR Aeronautics Design Challenge 2018-2019: Hintergrund und Design Anforderungen*. Ed. by DLR. 2018. URL: https://www.dlr.de/dlr/desktopdefault.aspx/tabid-10450/646_read-31391/#/gallery/32989.

[20] EASA: *TYPE-CERTIFICATE DATA SHEET: E.150 for RED A03 series engines: Type Certificate Holder; Raikhlin aircraft Engine Developments GmbH*. 2018. URL: https://www.easa.europa.eu/sites/default/files/dfu/EASA_E_150_TCDS_REDA03_issue%2002_20180827.pdf.

[21] EASA: "TYPE-CERTIFICATE DATA SHEET FOR NOISE: No. EASA.IM.A.226 for Cessna 208 (Caravan): Type Certificate Holder Textron Aviation Inc." In: (2018).

[22] FAA: *Advisory Circular*. 26.02.2014.

[23] Fieldin, John P. and Jemitola, Paul O.: "BOX WING AIRCRAFT CONCEPTUAL DESIGN". In: *28th International Congress Of The Aeronautical Sciences*. URL: http://www.icas.org/ICAS_ARCHIVE/ICAS2012/PAPERS/213.PDF.

[24] Gerhard Hüttig: *Enhanced Cockpit Visual and Flight Information System*. 2015. URL: https://www.ff.tu-berlin.de/menue/forschung/projektarchiv/ecovisfis/.

[25] GlobalTraveler.TV: *Emirates NEUE First Class Suiten, der Game Changer | GlobalTraveler.TV*. Ed. by YouTube. 2018. URL: https://www.youtube.com/watch?v=FWXtImwy9ew.

[26] God, Ralf: "Systems Engineering: Kapitel: Systems Engineering - Überblick". Vorlesung. Hamburg, Deutschland: Technische Universität Hamburg, 2019.

[27] Gollnick, Volker: "Luftfahrzeugentwurf I: Kapitel 11 - Kosten". Vorlesung. Hamburg, Deutschland: Technische Universität Hamburg, 2018.

[28] Gollnick, Volker: "Luftfahrzeugentwurf I: Kapitel 2 - Massenabschätzung". Vorlesung. Hamburg, Deutschland: Technische Universität Hamburg, 2018.

[29] Gollnick, Volker: "Luftfahrzeugentwurf I: Kapitel 3 - Rumpf und Kabine". Vorlesung. Hamburg, Deutschland: Technische Universität Hamburg, 2018.

[30] Handley, Mark: "Delay is Not an Option". In: *Proceedings of the 17th ACM Workshop on Hot Topics in Networks - HotNets '18*. Ed. by Unknown. New York, New York, USA: ACM Press, 2018, pp. 85–91. ISBN: 9781450361200. DOI: 10.1145/3286062.3286075.

[31] HAW: *Prediction of Drag*. 2017. URL: https://www.fzt.haw-hamburg.de/pers/Scholz/HOOU/AircraftDesign_13_Drag.pdf.

[32] Hepperle, Martin: "Aspects of Distributed Payload: A view on Regional Aircraft". In: *Symposium Elektrisches Fliegen*.

[33] Heron, Alex and Rinderknecht, Frank, eds.: *Comparison of Range Extender Technologies for Battery Electric Vehicles*. Piscataway, NJ: IEEE, 2013. ISBN: 9781467352710.

[34] Hitachi, Ltd.: *Hitachi Automotive Systems Delivers 5,000W/kg High Output Power Density Prismatic Lithium-ion Battery Cells for 2016 New Model GM Chevrolet Malibu Hybrid*. URL: www.hitachi.com/New/cnews/month/2015/05/150519a.pdf.

[35] Holt, Jon; Perry, Simon A., and Brownsword, Mike: *Model-based requirements engineering*. Vol. 9. IET Professional applications of computing series. Stevenage Herts U.K.: Institution of Engineering and Technology, 2012. ISBN: 9781849194884.

[36] Honeywell International Inc: *TYPE-CERTIFICATE DATA SHEET LTS101 series engines*. 2010. URL: https://www.easa.europa.eu/sites/default/files/dfu/EASA-TCDS-E.228_%28IM%29_Honeywell_International_Inc._LTS101_series_engines-04-19082010.pdf.

[37] Honeywell: *Air Data Inertial Reference System (ADIRS)*. 2007.

[38] *How to find the design angle of attack of my wing?* URL: https://www.mh-aerotools.de/airfoils/hdi_aoawing.htm.

[39] IATA: *Jet Fuel Price Monitor*. URL: https://www.iata.org/publications/economics/fuel-monitor/Pages/index.aspx.

[40] ICAO: *Annex 14 to thne Convention on International Civil Aviation: Volume 1 Aerodrome Design and Operations*. ISBN: 978-92-9258-483-2.

[41] Inigo del Portillo,Bruce G. Cameron, Edward F. Crawley: *A Technical Comparison of Three Low Earth Orbit Satellite Constellation Systems to Provide Global Broadband*. Bremen, 2018.

[42] Jack D. Stephenson: *NACA Split brakes*. Ed. by NACA. 1939.

[43] Jon Brodkin: *SpaceX hits two milestones in plan for low-latency satellite broadband*. 2018. URL: https://arstechnica.com/information-technology/2018/02/spacexs-satellite-broadband-nears-fcc-approval-and-first-test-launch/.

[44] Kadyk, Thomas; Winnefeld, Christopher, et al.: "Analysis and Design of Fuel Cell Systems for Aviation". In: *Energies* 11.2 (2018). DOI: 10.3390/en11020375.

[45] Kim, Hyun D.; Perry, Aaron T., and Ansell, Phillip J., eds.: *A Review of Distributed Electric Propulsion Concepts for Air Vehicle Technology*. 2018.

[46] Kroo, Ilan: *DRAG DUE TO LIFT: Concepts for Prediction and Reduction*. 2001.

[47] Krzysztof, Piwek: *D4.2 Operating Cost Analysis*. Ed. by European Personal Air Transportation System. 2007.

[48] Kusay-Merkle, Ursula: *Agiles Projektmanagement im Berufsalltag: Für mittlere und kleine Projekte*. Berlin: Springer Gabler, 2018. ISBN: 9783662567999. DOI: 10.1007/978-3-662-56800-2. URL: http://dx.doi.org/10.1007/978-3-662-56800-2.

[49] L. Schrittwieser, M. Leibl, M. Haider, F. Thöny, J.W. Kolar, T.B. Soeiro, ed.: *99.3% Efficient Three-Phase Buck-Type All-SiC SWISS Rectifier for DC Distribution Systems*. Tampa, FL, USA: IEEE, 2017. ISBN: 9781509053674.

[50] Langhans, Stephan: "A Systems Engineering Approach for Economic Assessment of Air Transportation Concepts". Forschungesbericht 2013-04. Hamburg, Deutschland: Technische Universität Hamburg, 2012.

[51] Ludowicy, J.; Rings, R., et al., eds.: *Sizing Studies of Light Aircraft with Serial Hybrid Propulsion Systems*. Deutsche Gesellschaft für Luft- und Raumfahrt - Lilienthal-Oberth e.V, 2018. DOI: 10.25967/480226.

[52] Mark Drela, Harold Youngren: *XFOIL 6.9 User Primer*. URL: https://web.mit.edu/drela/Public/web/xfoil/xfoil_doc.txt.

[53] Mark Plecity: *Inmarsat Aviation overview*. 2014. URL: http://www.inmarsat.com/wp-content/uploads/2014/06/07-GX_update-Mark_Plecity.pdf.

[54] Martin Holland: *SpaceX: FCC genehmigt Pläne für Satelliten-Internet Starlink*. 2018. URL: https://www.heise.de/newsticker/meldung/SpaceX-FCC-genehmigt-Plaene-fuer-Satelliten-Internet-Starlink-4009149.html.

[55] Martin, Billy M.: *Electromagnetic Effects and Composite Structure*. Ed. by National Institute for Aviation Research. n.d. URL: https://www.niar.wichita.edu/niarfaa/Portals/0/Electromagnetic%20Effects%20and%20Composite%20Structure%20-%20Billy%20Martin.pdf.

[56] Matt Thurber: *FAA, EASA OK Dassault 8X EFVS Down to 100 Feet*. 2018. URL: https://www.ainonline.com/aviation-news/business-aviation/2018-10-09/faa-easa-ok-dassault-8x-efvs-down-100-feet.

[57] McDonald, Colin F.; Massardo, Aristide F., et al.: "Recuperated gas turbine aeroengines. Part III: engine concepts for reduced emissions, lower fuel consumption, and noise abatement". In: *Aircraft Engineering and Aerospace Technology* 80.4 (2008), pp. 408–426. ISSN: 0002-2667. DOI: 10.1108/00022660810882773.

[58] Megginson, David: *OurAirports: For people who fly*. URL: http://ourairports.com/.

[59] Mielke, Daniel M.: "C-Band Digital Aeronautical Communication for Unmanned Aircraft Systems". In: *AIAA/IEEE Digital Avionics Systems Conference - Proceedings. DASC 2017*, 17.–21. Sep. 2017.

[60] Mirus Aircraft Seating: *mirus vision 2030*. URL: www.mirus-as.com.

[61] Moir, I. and Seabridge, A. G.: *Aircraft systems: Mechanical, electrical, and avionics subsystems integration*. 3rd ed. Aerospace series. Chichester West Sussex England and Hoboken NJ: Wiley, 2008. ISBN: 0470059966.

[62] Moir, I.; Seabridge, A. G., and Jukes, Malcolm: *Civil avionic systems*. 2nd edition. Chichester West Sussex: Wiley, 2013. ISBN: 9781118536742.

[63] Nabel, abd-ali and Ahmed, Raee: "Effect of Fiber Orientation Angles on Mechanical Behavior of Car Bumper Composite". In: *Engineering KUFA Journal* (10.2016).

[64] NASA: *NASA University Engineering Design Challenge, 2018-2019*. URL: https://aero.larc.nasa.gov/university-contest/2018-2019_challenge_final_2018-09-04/.

[65] Ozve Aminian, Negin and Izzuddin Romli, Fairuz: "Ergonomics assessment of current aircraft passenger seat design against Malaysian anthropometry data". In: *International Journal of Engineering & Technology* 7.4.13 (2018), pp. 18–21. DOI: 10.14419/ijet.v7i4.13.21322.

[66] Pagano, Antonio; Barbarino, Mattia, et al.: "Tonal and Broadband Noise Calculations for Aeroacoustic Optimization of a Pusher Propeller". In: *Journal of Aircraft* 47.3 (2010), pp. 835–848. ISSN: 0021-8669. DOI: 10.2514/1.45315.

[67] Petermaier, Korbinian, ed.: *Electric propulsion components with high power densities for aviation*. 2105.

[68] Pieper, Kyle C.; Perry, Aaron T., et al., eds.: *Design and Development of a Dynamically Scaled Distributed Electric Propulsion Aircraft Testbed*. July 9-11, 2018. DOI: 10.2514/6.2018-4996.

[69] R. H. Lange et al.: "FEASIBILITY STUDY OF THE TRANSONIC BIPLANE CONCEPT FOR TRANSPORT AIRCRAFT APPLICATION". In: (Juni 1974).

[70] R. SC-228: *Rtca paper no. 075-14/pmc-1201: Command and control (c2) data link white paper*. 2014.

[71] Raymer, Daniel P.: *Aircraft design: A conceptual approach*. 4. ed. AIAA education series. Reston, Va.: American Institute of Aeronautics and Astronautics, 2006. ISBN: 9781563478291.

[72] Raymer, Daniel P.: *Aircraft design: A conceptual approach*. 5. ed. AIAA education series. Reston, Va.: AIAA American Inst. of Aeronautics and Astronautics, 2012. ISBN: 9781600869112.

[73] Redondo-Iglesias, Eduardo; Venet, Pascal, and Pelissier, Serge: "Efficiency Degradation Model of Lithium-ion Batteries for Electric Vehicles". In: *IEEE Transactions on Industry Applications* (2019). URL: https://hal.archives-ouvertes.fr/hal-01898906/document.

[74] Richter, Thomas: *100 kW SiC-Inverter for Automotive Application*. URL: https://www.iisb.fraunhofer.de/content/dam/iisb2014/en/Documents/Research-Areas/vehicle_electronics/2017-05-08_FraunhoferIISB_Produktblatt_100kW-SiC-Inverter_WWW.pdf.

[75] Rinderknecht, Frank: "Entwicklung und Untersuchung eines Lineargenerators für ein Hybridfahrzeug". Dissertation. Technische Universität München, 2009.

[76] Sam Chui: *EMIRATES NEW 2018 FIRST CLASS - IT'S A 5* HOTEL!!!* Ed. by YouTube. 2018. URL: https://www.youtube.com/watch?v=nSOG99qClU8.

[77] Schmitt, Dieter and Gollnick, Volker: *Air Transport System*. 1st ed. 2016. Wien: Springer, 2016. ISBN: 978-3-7091-1880-1. DOI: 10.1007/978-3-7091-1880-1.

[78] Scholz, Dieter: *Aircraft Design - Fuselage Design*. Ed. by Hamburg University of Applied Sciences. 2015. URL: https://www.fzt.haw-hamburg.de/pers/Scholz/HOOU/AircraftDesign_6_Fuselage.pdf.

[79] Siemens AG: *Factsheet: Rekord-Motor SP260D und Extra 330LE*. URL: https://www.siemens.com/press/pool/de/feature/2015/corporate/2015-03-electromotor/factsheet-erstflug-weltrekordmotor-d.pdf.

[80] SpaceX: *Starlink constellation*. 2017. URL: https://www.starlink.com/.

[81] Spitzer, Cary R.; Ferrell, Uma, and Ferrell, Thomas, eds.: *Digital avionics handbook*. Third edition. Boca Raton, London, and New York: CRC Press, 2015. ISBN: 9781439868614. DOI: 10.1201/b17545-47. URL: http://dx.doi.org/10.1201/b17545-47.

[82] Sporty's Pilot Shop, ed.: *Little John Pilot Urinal*. URL: https://www.sportys.com/pilotshop/little-john-pilot-urinal.html.

[83] Stahl, Philipp; Roessler, Christian, and Hornung, Mirko: *Configuration Redesign and Prototype Flight Testing of an Unmanned Fixed-Wing eVTOL Aircraft with Under-Fuselage Hover Lift and Pusher Wingtip Propulsion System*. 2019. URL: https://www.researchgate.net/publication/331113931.

[84] Stoll, Alex M., ed.: *Design Studies of Thin-Haul Commuter Aircraft with Distributed Electric Propulsion*. 2016.

[85] stroh, anne: "Potenzial zukünftiger Hubschrauber-Triebwerke der 300 kW-Leistungsklasse durch Einsatz optimierter rekuperativer Systeme". Dissertation. Technische Universität München, 2015.

[86] Textron Aviation, ed.: *Cessna Caravan: THE ORIGINAL TRAILBLAZER*. 2019. URL: https://cessna.txtav.com/en/turboprop/caravan.

[87] *The Future of the NAS*. June 2016. URL: https://www.faa.gov/nextgen/media/futureOfTheNAS.pdf.

[88] Thielecke, F.: "Klimaanlagen - Kapitel 1: Klimaanlagen und Bordkühlsysteme". PhD thesis. Hamburg, Deutschland: Technische Universität Hamburg, 2018.

[89] U.S. Department of Transportation, ed.: *Essential Air Service: Current and Historical Status Reports and links to other EAS Reports and Publications*. Transportation.gov, 22.11.2017. URL: https://www.transportation.gov/policy/aviation-policy/small-community-rural-air-service/essential-air-service.

[90] U.S. Government, ed.: *Electronic Code of Federal Regulations: Title 14: Aeronautics and Space, PART 23—AIRWORTHINESS STANDARDS: NORMAL CATEGORY AIRPLANES*. 2019. URL: https://www.ecfr.gov/cgi-bin/text-idx?SID=685dc1ae97ae3f5e5569e47880fab01e&mc=true&node=pt14.1.23.

[91] Wittmann, R.: "PASSENGER ACCEPTANCE OF BWB CONFIGURATIONS". In: *International Congress of the Aeronautical Sciences* (2004).

A Technical Design

A.1 Aerodynamics

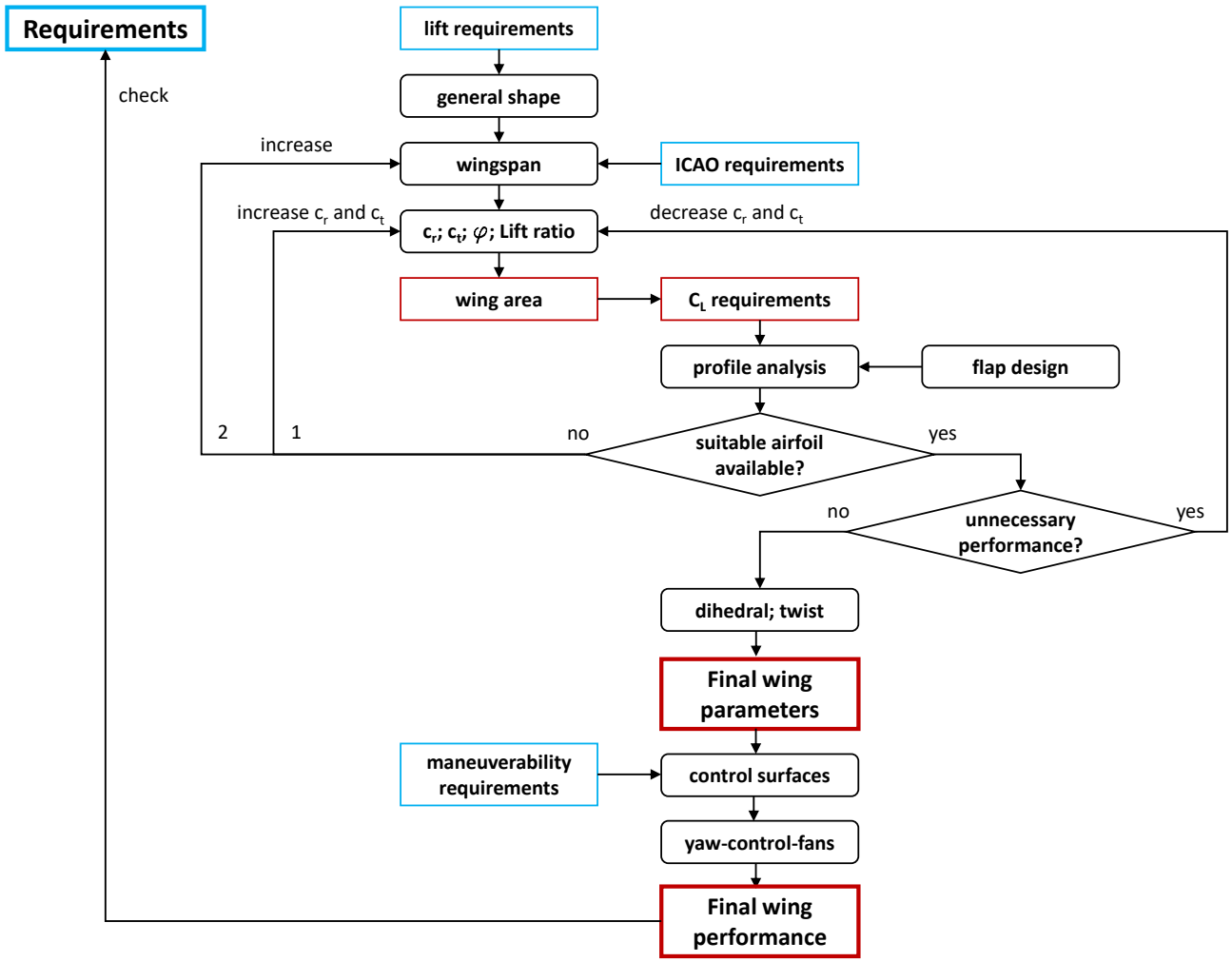

Figure A.1: Wing design process

Mesh setup	
Element sizes	
Inlet	2,2 m
Outlet	0,95 m
Interfaces	00,44 m
Fuselage	0,095 m
Inflation Option	last aspect ratio
First layer height	0,095 m
Maximum Layers	1000
FLUENT setup	
Friction Model	Spalart-Allmaras
Material	Air according to ISA
Inlet velocity	According to the flight phase
Solution method	Green-Gauss Node Based
Convergence criterion	$1 \cdot 10^{-06}$ for all residuals
Iterations	3000

Table A.1: Settings used for CFD-software ANSYS FLUENT as recommended by [4]

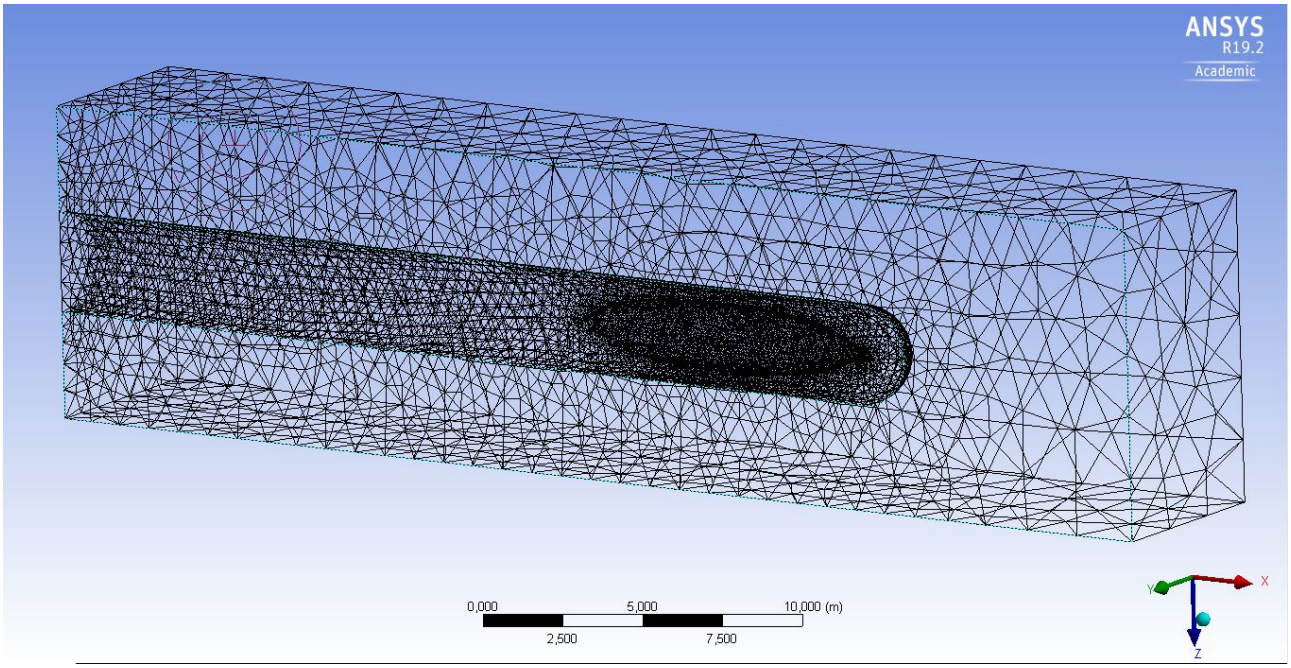

Figure A.2: Meshing results for CFD analysis of fuselage with ANSYS FLUENT

B.2 Avionics

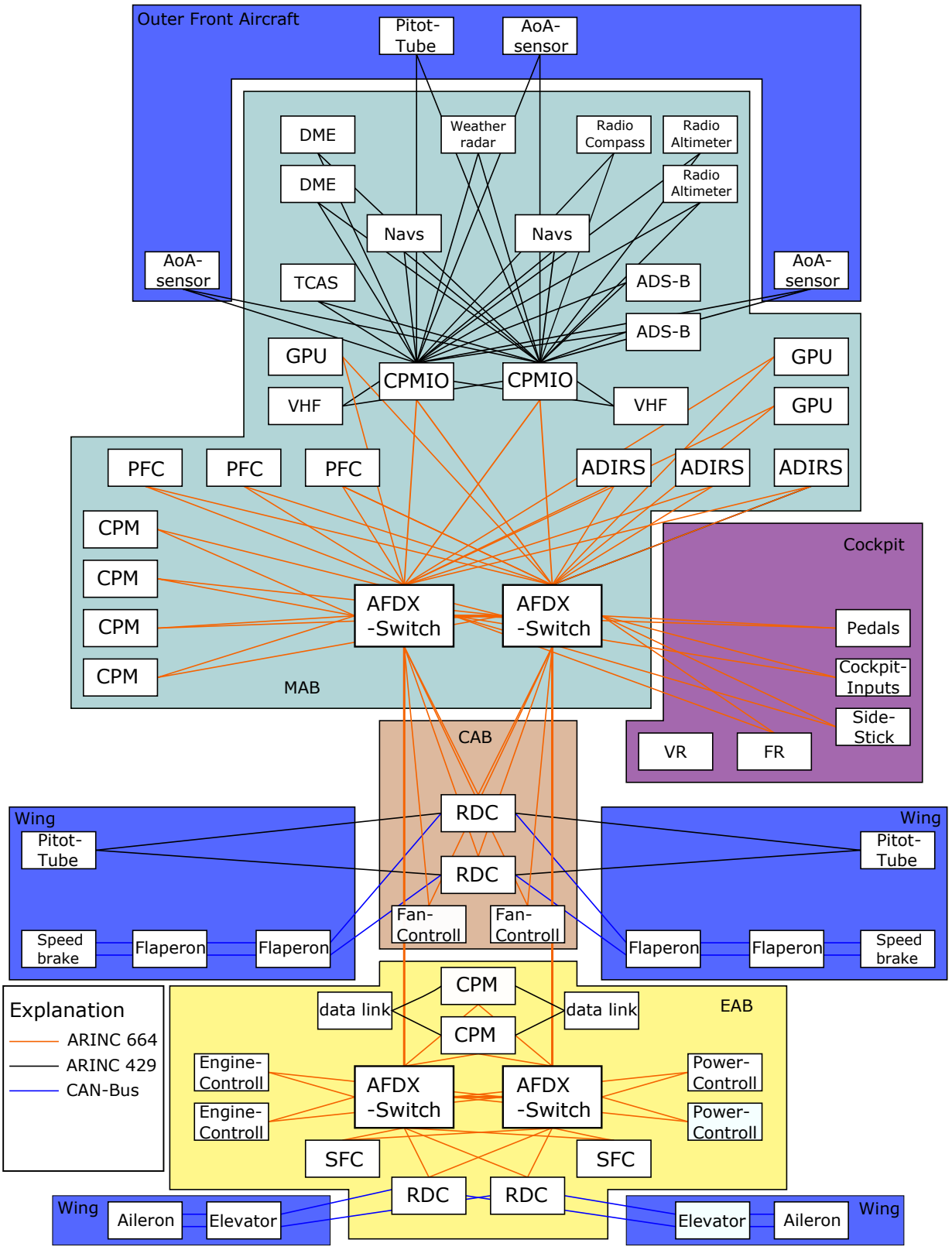

Figure A.3: Overview of avionics configuration

C.3 Cockpit

Figure A.4: Main view of the Cockpit

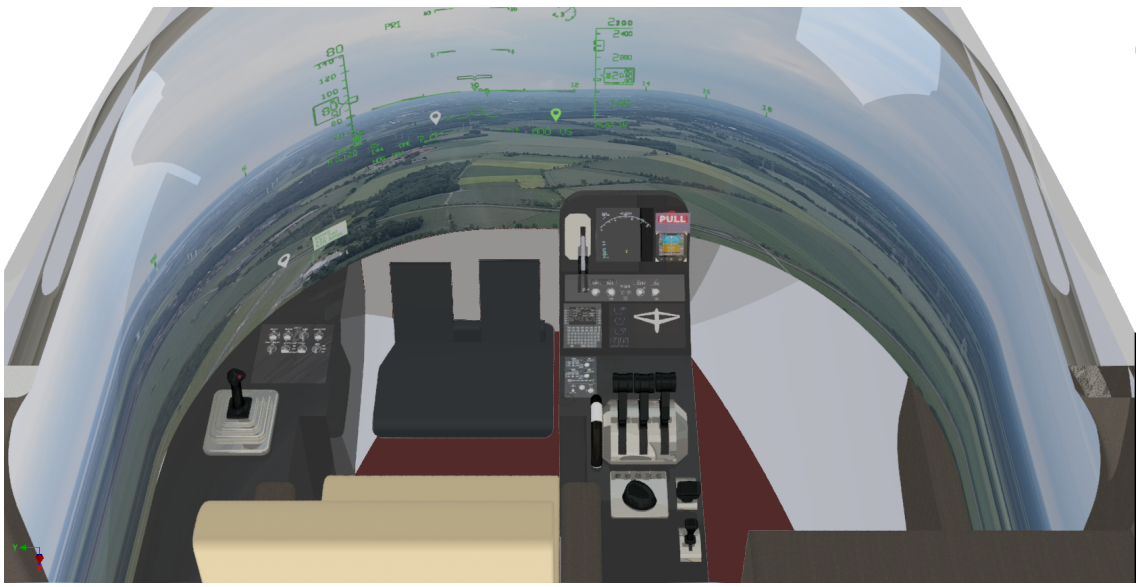

Figure A.5: View of the cockpits display

D.4 Cabin

Figure A.6: View into cabin: left side

Figure A.7: View into cabin: right side

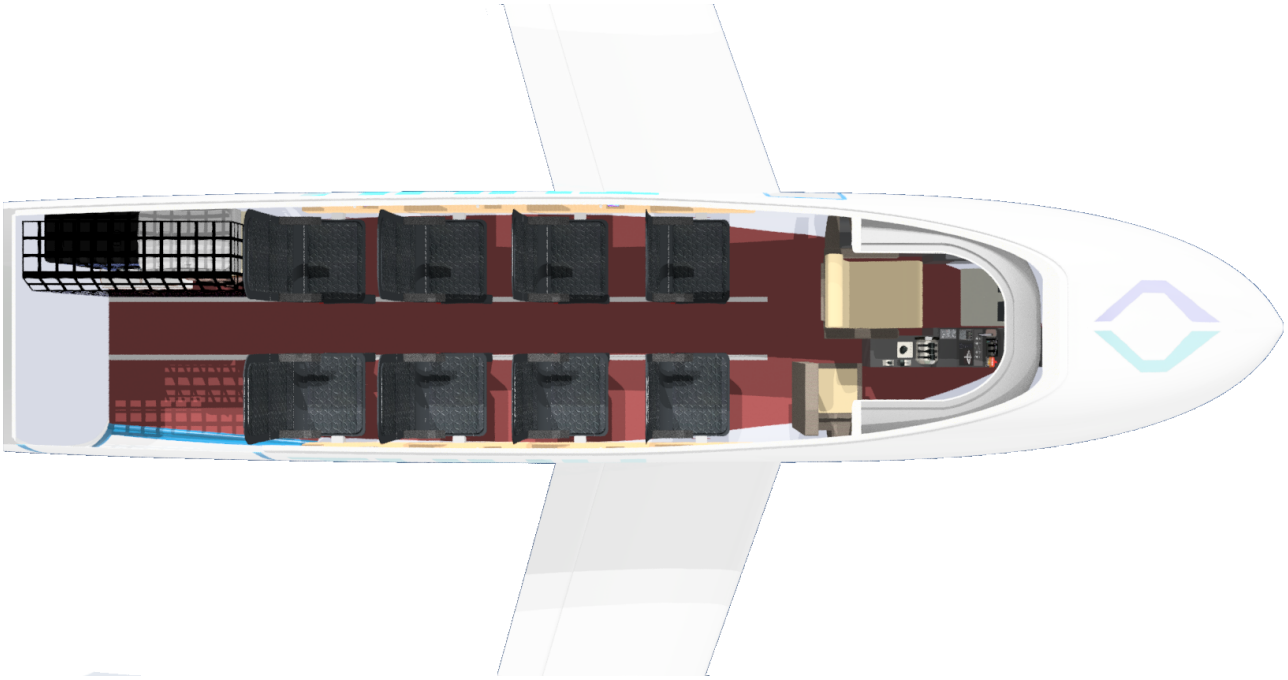

Figure A.8: View into cabin: top view

OLEDs	canopy
+ no direct incident solar radiation	+ can be used as an emergency exit
+ pilot can sit anywhere	→ only 2 emergency exits necessary
+ less structural weight	+/- freight loaded through the canopy
→ less fuel	- direct incident solar radiation
→ less costs	→ blinds or any technique which prevents
→ less emission of CO_2	the pilot to be dazzled and the cabin
→ longer ranges possible	to heat up is needed
→ shorter runways needed	- damage while (dis)assembling the
+ additional functions e.g. augmented reality	equipment possible
∘ passenger acceptance chapter 4.6.3)	→ aircraft might get grounded more often
- cameras needed	
- 3 emergency exits necessary (chapter 4.6.1)	
- power needed for screens	

Table A.2: OLED windows vs. canopy window

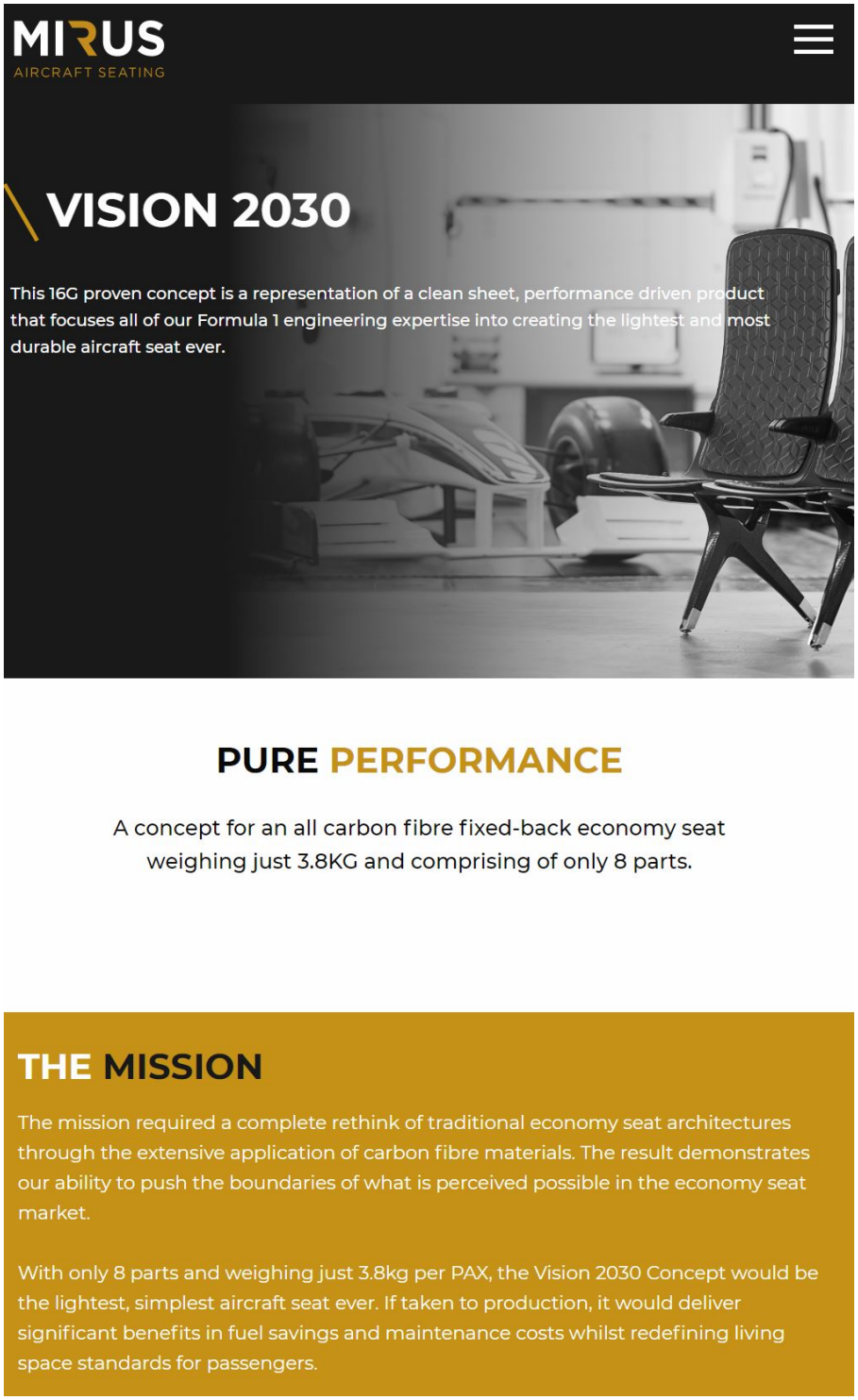

Figure A.9: Mirus Aircraft Seat Vision 2030 data sheet taken from Mirus Aircraft Seating [60]

B Flight Performance

System	Value	Unit
Fuselage	550	kg
Wings	350	kg
LDG & wheel engine	180	kg
EDFs	120	kg
Cruise propeller	50	kg
Motor	50	kg
Generator	50	kg
Turbine	120	kg
Fuel system	15	kg
Power electronics (incl. wiring)	50	kg
Battery	100	kg
Avionics mass	220	kg
Actuator	140	kg
Emergency parachute	20	kg
Cockpit	70	kg
Cabin	130	kg
AC	40	kg
OME	2255	kg
Payload	997.9	kg
Fuel mass	285.4	kg
MTOM	3538.3	kg

Table B.1: Detailed mass division

C Operations and Costs

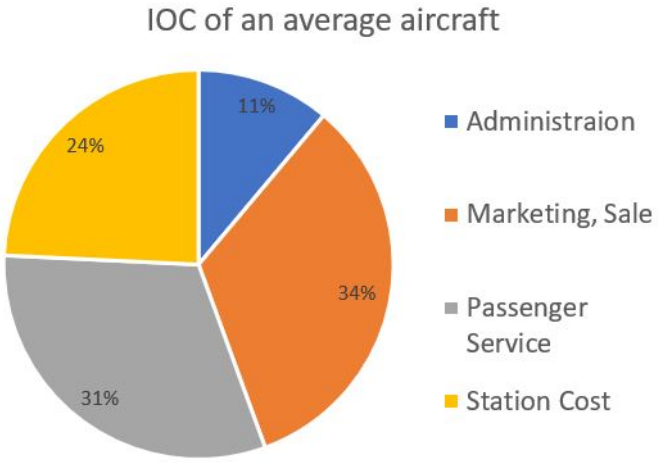

Figure C.1: Commonly IOC distribution of aircaft

The following table shows the estimated total operating costs per nautical mile for a 100 nm flight in 2018 USD. The data for the Cessna 208 are taken from Stoll [84].
The amount for overhaul and maintenance of the rAPID is comparable to high lift propellers which data were also presented in Stoll [84]. Fuel price of the rAPID is calculated with Breguet's formula. Ownership is based on the aircraft's price. Therefore the percentage of the ownership costs of the Cessna 208 data was taken to evaluate it for the rAPID. The pilot's costs for the rAPID are set a bit lower due to the avionics. Insurance is also based on the aircraft's price (1 % of it per year). Landing fees are set to 4 USD per 1000 lb of MTOM.

	Cessna 402	rAPID
overhaul & maintenance	1.9	1
fuel	0.85	0.68
ownership	0.5	0.85
pilot	0.55	0.495
insurance	0.05	0.075
landing fees	0.3	0.3
	4.10	3.40

Table C.1: Direct Operating Cost Evaluation